Supporting Information

Structure Determination Using the Method of Continuous Variations: Lithium Phenolates Solvated by Protic and Dipolar Aprotic Ligands

Laura Tomasevich and David B. Collum*

Contribution from the Department of Chemistry and Chemical Biology
Baker Laboratory, Cornell University
Ithaca, New York 14853-1301

X_A = the mole fraction of phenolate subunits **A**

X_B = the mole fraction of phenolate subunits **B**

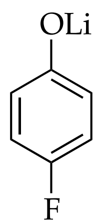

1

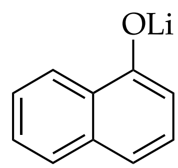

2

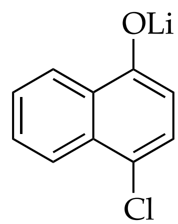

9

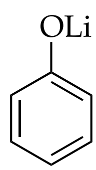

8

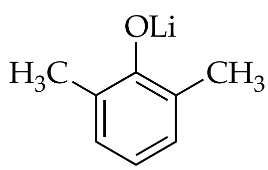

3

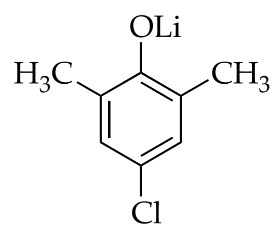

4

I. Combinations of phenolates with various solvents: Job plots.

For a full list of Job plots and their corresponding page numbers, please refer to pages S2-S6.

II. Solvent swaps.

For a full list of solvent swaps and their corresponding page numbers, please refer to page S7.

I. Combinations of lithium phenolates with various solvents: Job plots.

Substrate	Solvent	Structure(s)	Page
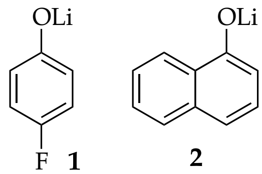 1, 2	TMEDA	dimer	S8
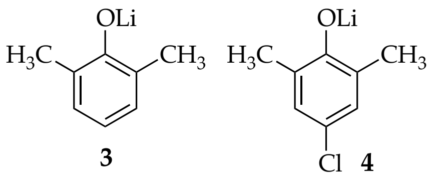 3, 4		dimer	S9
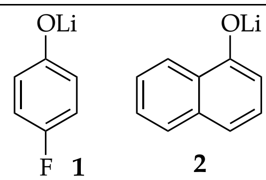 1, 2	Et_2O	tetramer	5 equiv-S10 neat-S11
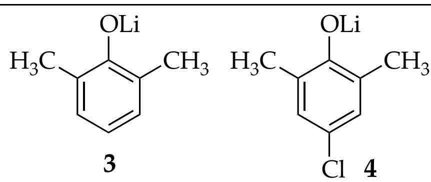 3, 4		trimer	S12
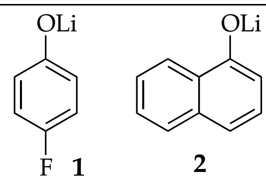 1, 2	MeCN	tetramer	S13
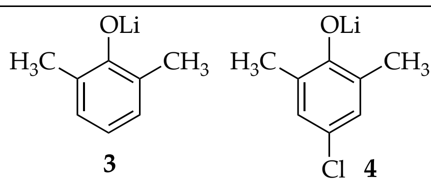 3, 4		tetramer	S14
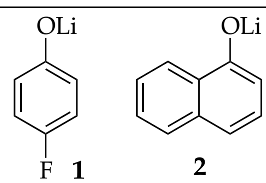 1, 2	pyridine	tetramer	S15
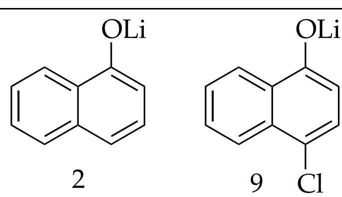 2, 9		tetramer	S16

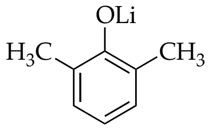 3 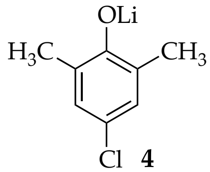 4	pyridine	dimer	S17
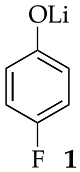 1 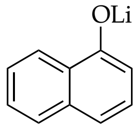 2	DMA	tetramer	S18
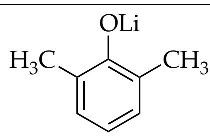 3 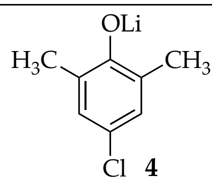 4		tetramer	S19
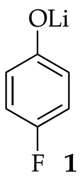 1 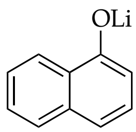 2	DMF	tetramer	S20
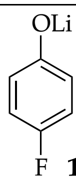 1 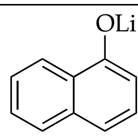 2	DMSO	tetramer	^{6}Li-S21 ^{19}F-S22
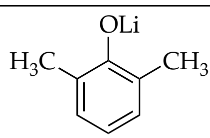 3 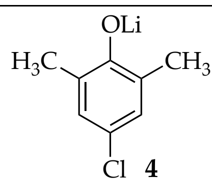 4		trimer and tetramer	S23
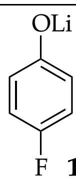 1 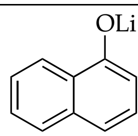 2	DMPU	tetramer	S24
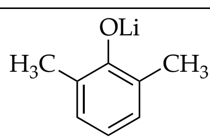 3 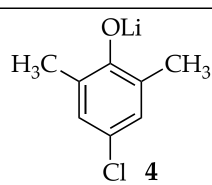 4		fast inter- and intra-aggregate exchange	S25
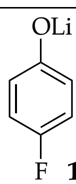 1 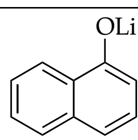 2	NMP	tetramer	S26

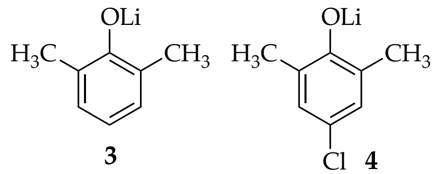 3, 4	NMP	tetramer	S27
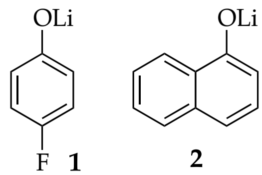 1, 2	n-PrNH$_2$	tetramer	S28
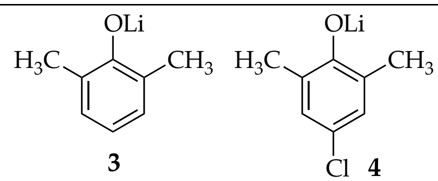 3, 4		dimer	S29
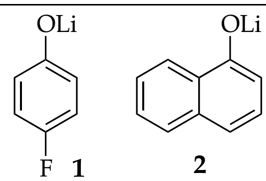 1, 2	piperidine	tetamer	^{6}Li-S30 ^{19}F-S31
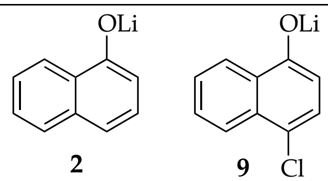 2, 9		trimer	S32
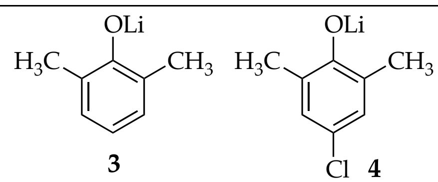 3, 4		dimer	S33
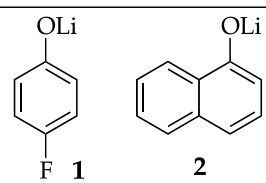 1, 2	pyrrolidine	tetramer	S34
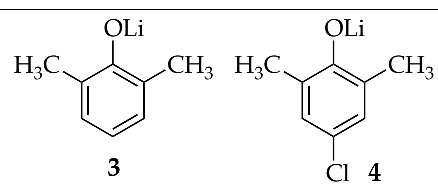 3, 4		dimer	S35

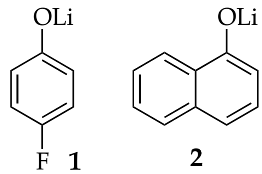 1, 2	i-$BuNH_2$	tetramer	S36
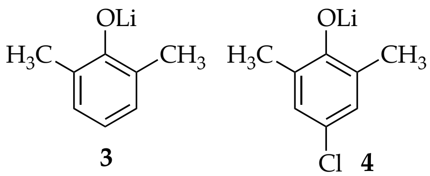 3, 4		dimer	S37
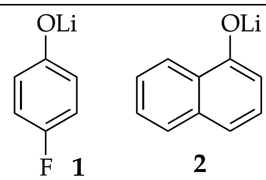 1, 2	*sec*-$BuNH_2$	tetramer	S38
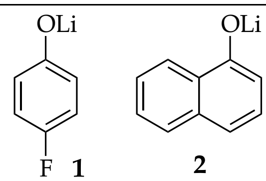 1, 2	t-$BuNH_2$	tetramer	S39
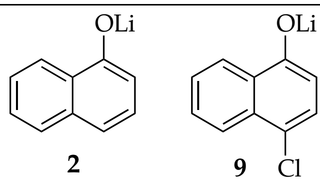 2, 9	(i-Pr)$_2$NH	trimer	S40
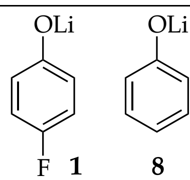 1, 8		Does not form hetero aggregates	S41
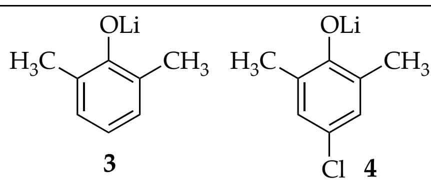 3, 4		dimer	S42
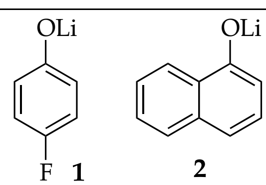 1, 2	Et_2NH	tetramer	S43
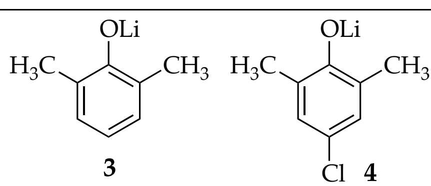 3, 4		trimer	S44

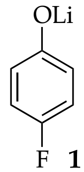 1 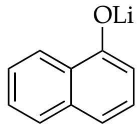 2	n-Pr_2NH	tetramer	S45
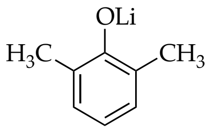 3 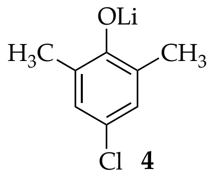 4		trimer	S46
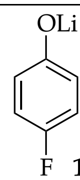 1 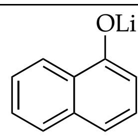 2	t-BuOH	tetramer	S47
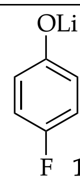 1 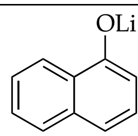 2	*sec*-BuOH	tetramer	S48
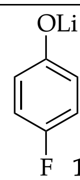 1 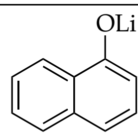 2	n-BuOH with toluene as cosolvent	fast inter- and intra-aggregate exchange	S49
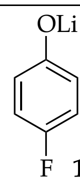 1 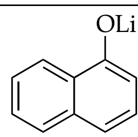 2	n-BuOH with Et_2O as cosolvent	tetramer	

II. Solvent Swaps

Substrate	Solvent 1	Solvent 2	Page
1	Pyridine	Et_2NH	S50
2	Et_2NH	TMEDA	S51
1	DMA	TMEDA	S52
1	DMF	TMEDA	S53
1	NMP	TMEDA	S54
1	NMP	TMEDA	S55
1	Pyridine	NMP	S56
1	Pyridine	NMP	S57
1	Pyridine	Et_2O	S58
1	Pyridine	Et_2O	S59
1	Pyridine	Et_2O	S60
1	Pyridine	TMEDA	S61
1	Pyridine	TMEDA	S62
2	Pyridine	TMEDA	S63
1	Pyridine	*n*-$PrNH_2$	S64
1	Pyridine	Pyrrolidine	S65
1	Pyridine	*t*-BuOH	S66

Dimer Job Plots in TMEDA

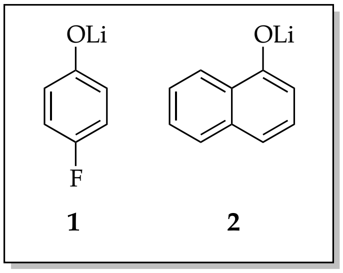

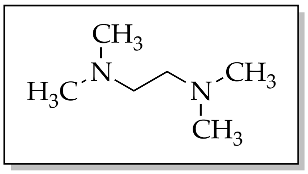

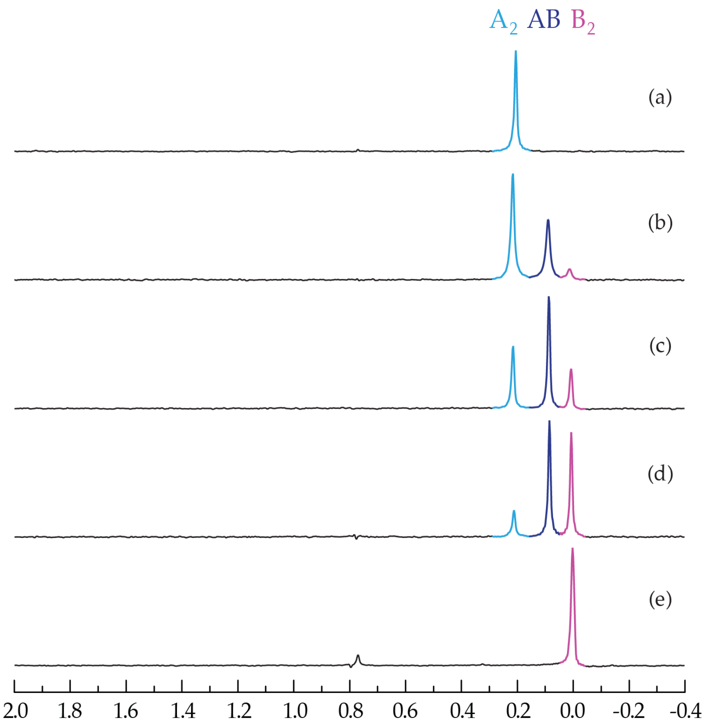

Figure 1. ^{6}Li NMR spectra of 0.10 M solutions of [^{6}Li]**2** (**A**) and [^{6}Li]**1** (**B**) in 0.50 M $(CH_3)_2NCH_2CH_2N(CH_3)_2$/toluene at -90 °C. The measured mole fractions of **A** in (a)-(e) are 1.00, 0.74, 0.56, 0.25, and 0.00, respectively.

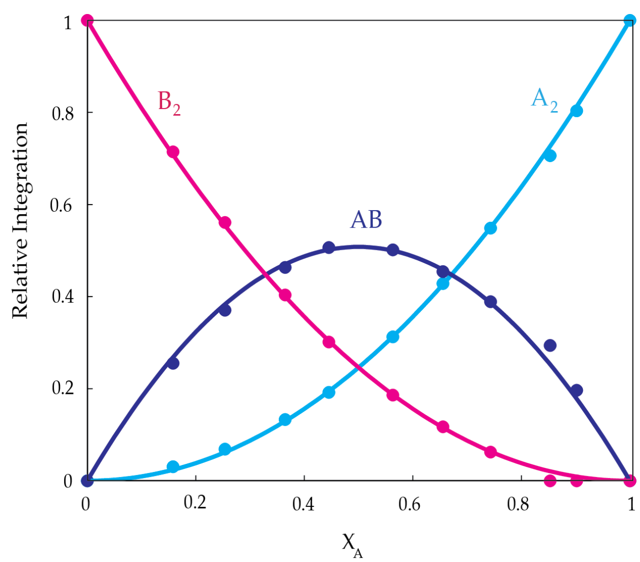

Figure 2. Job plot showing the relative integrations versus the measured mole fractions of **2** for 0.10 M mixtures of [^{6}Li]**2** (**A**) and [^{6}Li]**1** (**B**) in 0.50 M $(CH_3)_2NCH_2CH_2N(CH_3)_2$/toluene at -90 °C.

Dimer Job Plots in TMEDA

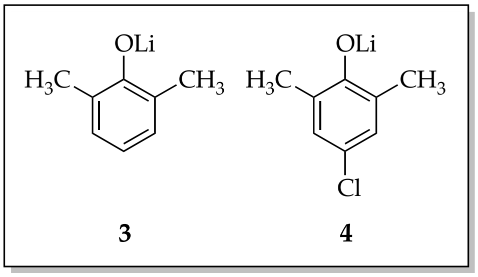

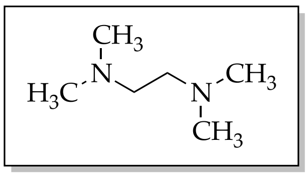

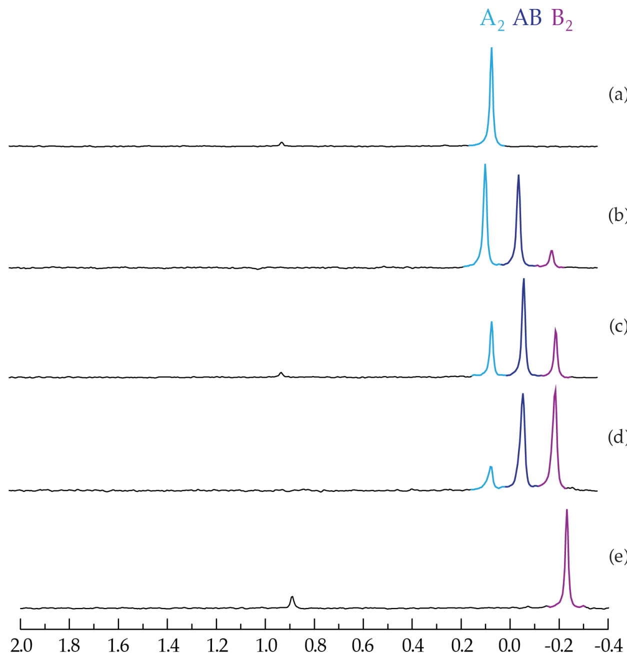

Figure 3. ^{6}Li NMR spectra of 0.10 M solutions of [^{6}Li]**3** (**A**) and [^{6}Li]**4** (**B**) in 0.50 M $(CH_3)_2NCH_2CH_2N(CH_3)_2$/toluene at -80 °C. The measured mole fractions of **A** in (a)-(e) are 1.00, 0.66, 0.48, 0.30, and 0.00, respectively.

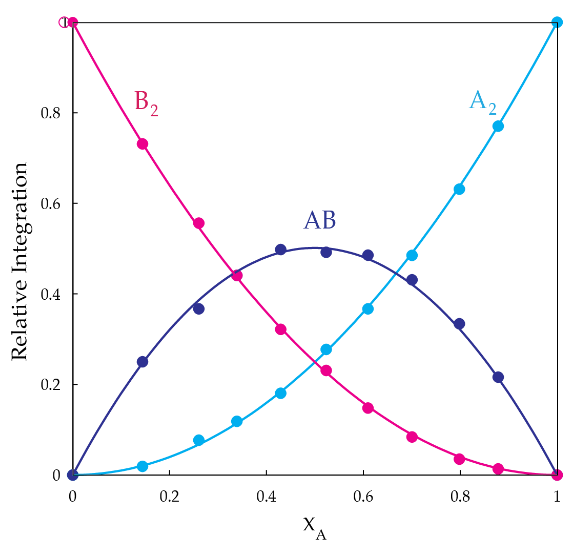

Figure 4. Job plot showing the relative integrations versus the measured mole fractions of **3** for 0.10 M mixtures of [^{6}Li]**3** (**A**) and [^{6}Li]**4** (**B**) in 0.50 M $(CH_3)_2NCH_2CH_2N(CH_3)_2$/toluene at -80 °C.

Tetramer Job Plots in Diethyl Ether

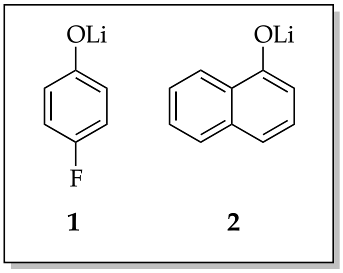

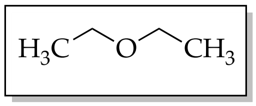

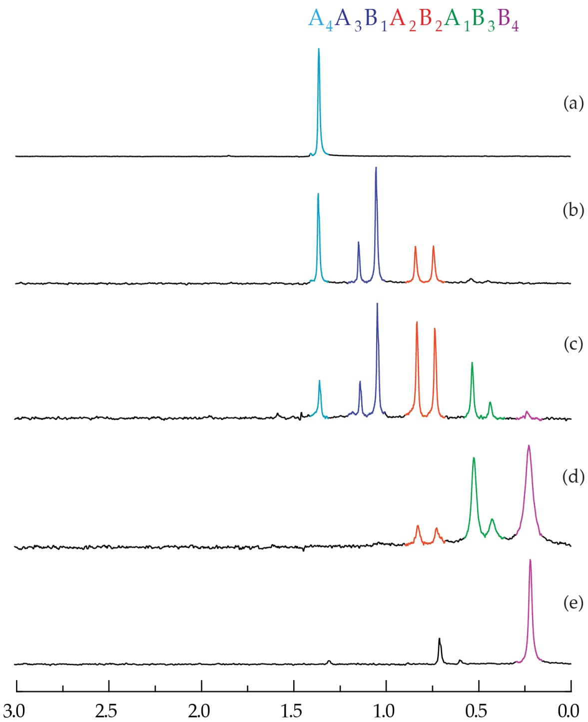

Figure 5. ^{6}Li NMR spectra of 0.10 M solutions of [^{6}Li]**2** (**A**) and [^{6}Li]**1** (**B**) in 0.50 M Et_2O/toluene at -90°C. The measured mole fractions of **A** in (a)-(e) are 1.00, 0.70, 0.43, 0.17, and 0.00, respectively.

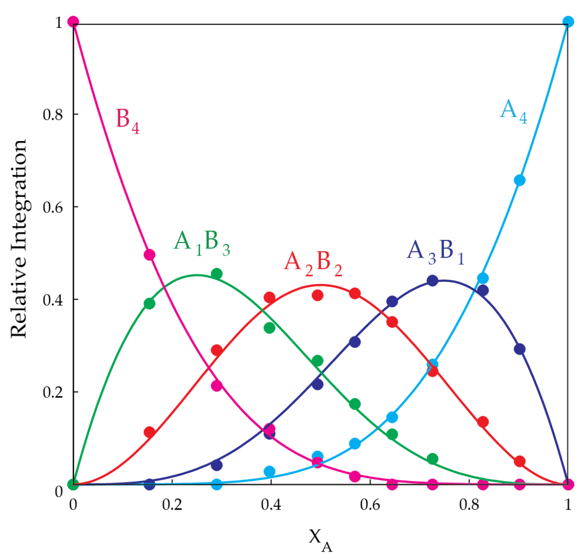

Figure 6. Job plot showing the relative integrations versus the measured mole fractions of **2** for 0.10 M mixtures of [^{6}Li]**2** (**A**) and [^{6}Li]**1** (**B**) in 0.50 M Et_2O/toluene at -90 °C.

<u>**Tetramer Job Plots in Diethylether**</u>

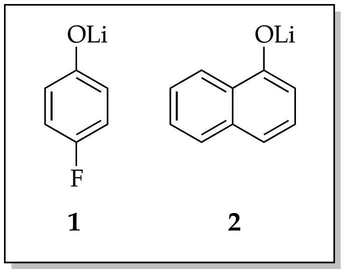

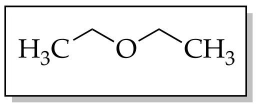

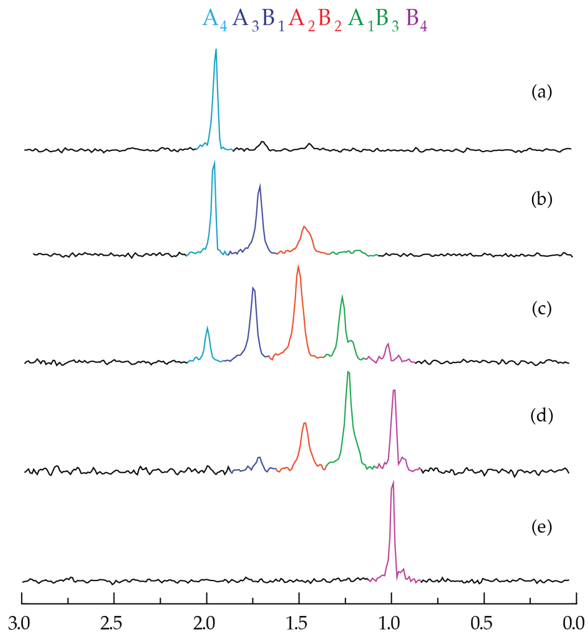

Figure 7. [6]Li NMR spectra of 0.10 M solutions of [^{6}Li]**2** (**A**) and [^{6}Li]**1** (**B**) in neat Et_2O at +22 °C. The measured mole fractions of **A** in (a)-(e) are 1.00, 0.72, 0.48, 0.25, and 0.00, respectively.

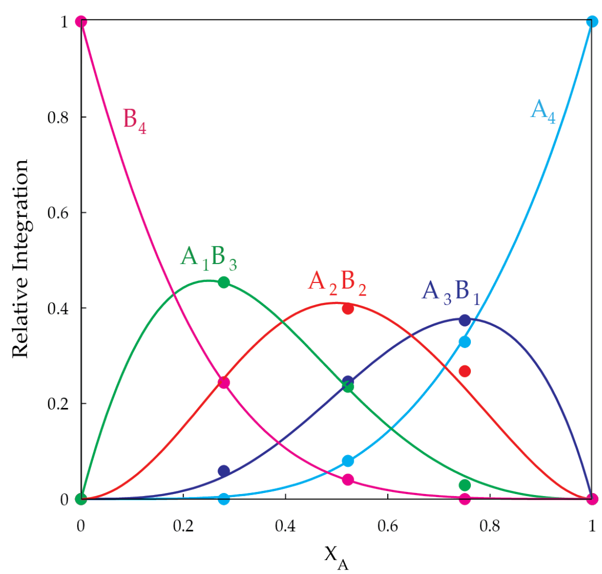

Figure 8. Job plot showing the relative integrations versus the measured mole fractions of **2** for 0.10 M mixtures of [^{6}Li]**2** (**A**) and [^{6}Li]**1** (**B**) in 0.50 M Et_2O/toluene at +22 °C.

<u>**Trimer Job Plots in Diethylether**</u>

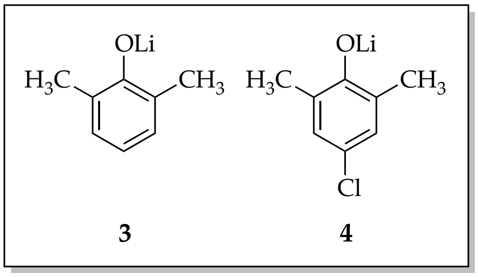

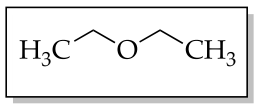

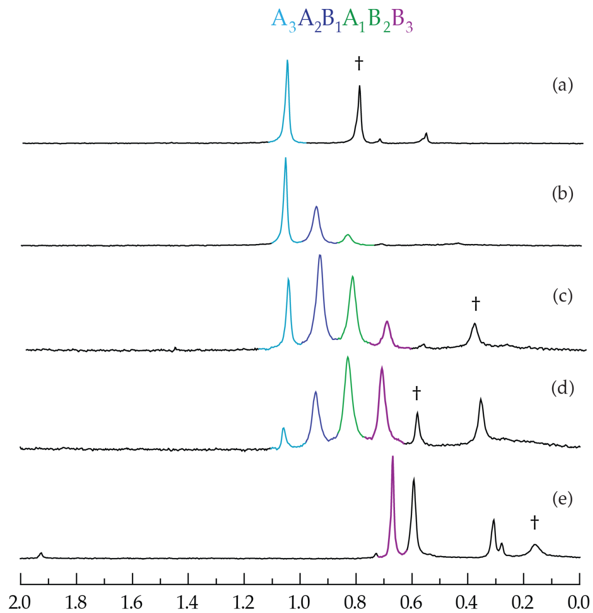

Figure 9. ^{6}Li NMR spectra of 0.10 M solutions of [^{6}Li]**3** (**A**) and [^{6}Li]**4** (**B**) in 0.50 M Et_2O/toluene at -90°C. The measured mole fractions of **A** in (a)-(e) are 1.00, 0.86, 0.54, 0.32, and 0.00, respectively. † indicates unknown aggregate.

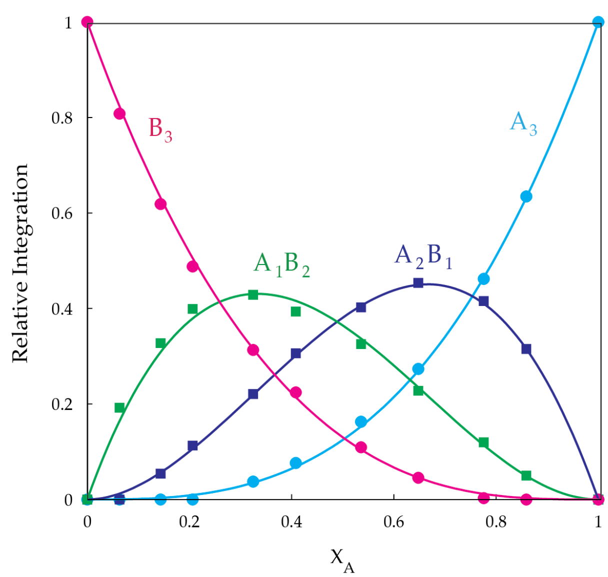

Figure 10. Job plot showing the relative integrations versus the measured mole fractions of **3** for 0.10 M mixtures of [^{6}Li]**3** (**A**) and [^{6}Li]**4** (**B**) in 0.50 M Et_2O/toluene at -90 °C.

Tetramer Job Plots in Acetonitrile

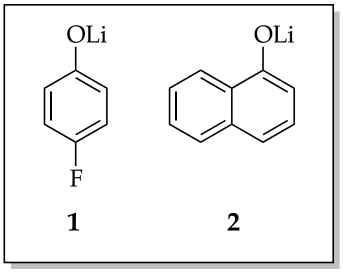

$H_3C-C\equiv N$

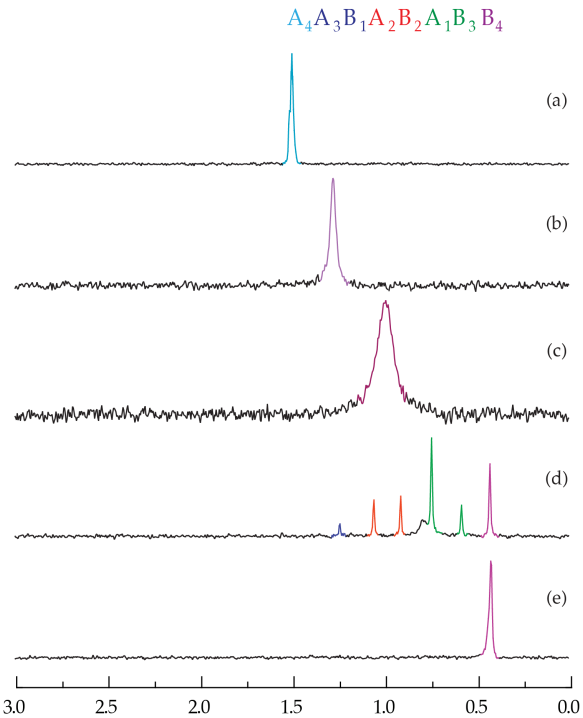

Figure 11. ^{6}Li NMR spectra of 0.10 M solutions of [^{6}Li]**2** (**A**) and [^{6}Li]**1** (**B**) in 0.50 M H_3CCN/toluene at -80 °C. The mole fractions of **A** in (a)-(e) are roughly 1.00, 0.75, 0.50, 0.25, and 0.00, respectively. The intermolecular exchange rate is fast except for when the ratio of **1** to **2** is 3:1.

Tetramer Job Plots in Acetonitrile

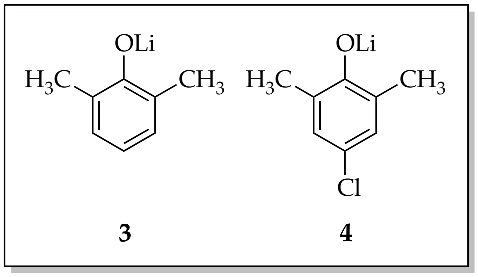

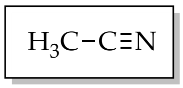

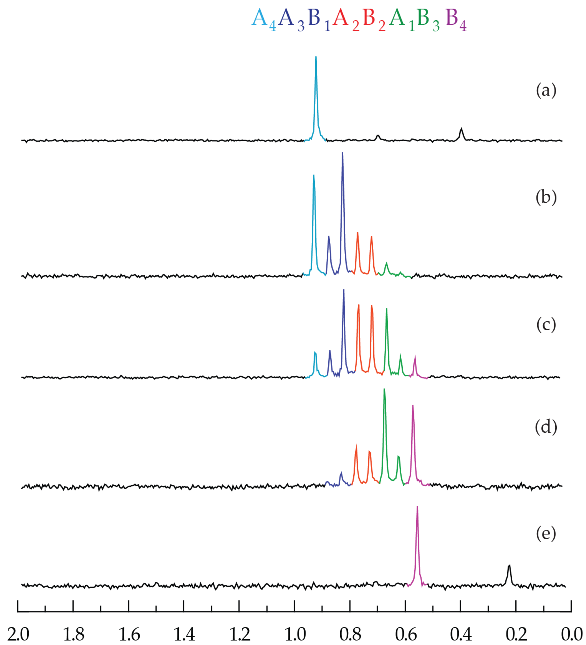

Figure 12. ^{6}Li NMR spectra of 0.10 M solutions of [^{6}Li]**3** (**A**) and [^{6}Li]**4** (**B**) in 0.50 M H_3CCN/toluene at -80 °C. The measured mole fractions of **A** in (a)-(e) are 1.00, 0.71, 0.47, 0.27, and 0.00, respectively.

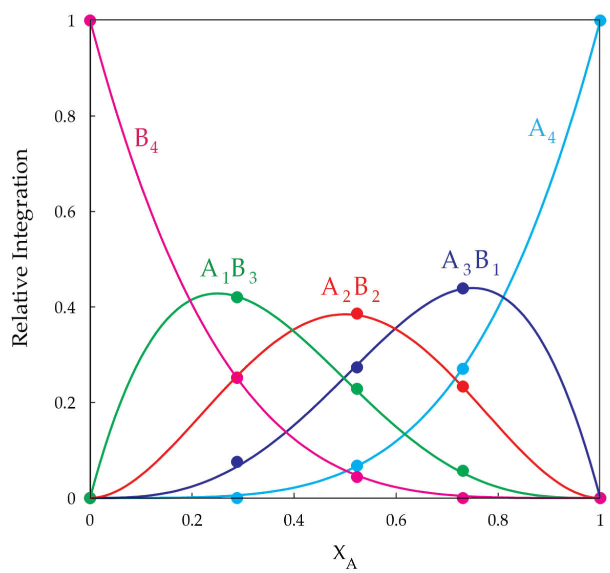

Figure 13. Job plot showing the relative integrations versus the measured mole fractions of **3** for 0.10 M mixtures of [^{6}Li]**3** (**A**) and [^{6}Li]**4** (**B**) in 0.50 M H_3CCN/toluene at -80 °C.

Tetramer Job Plots in Pyridine

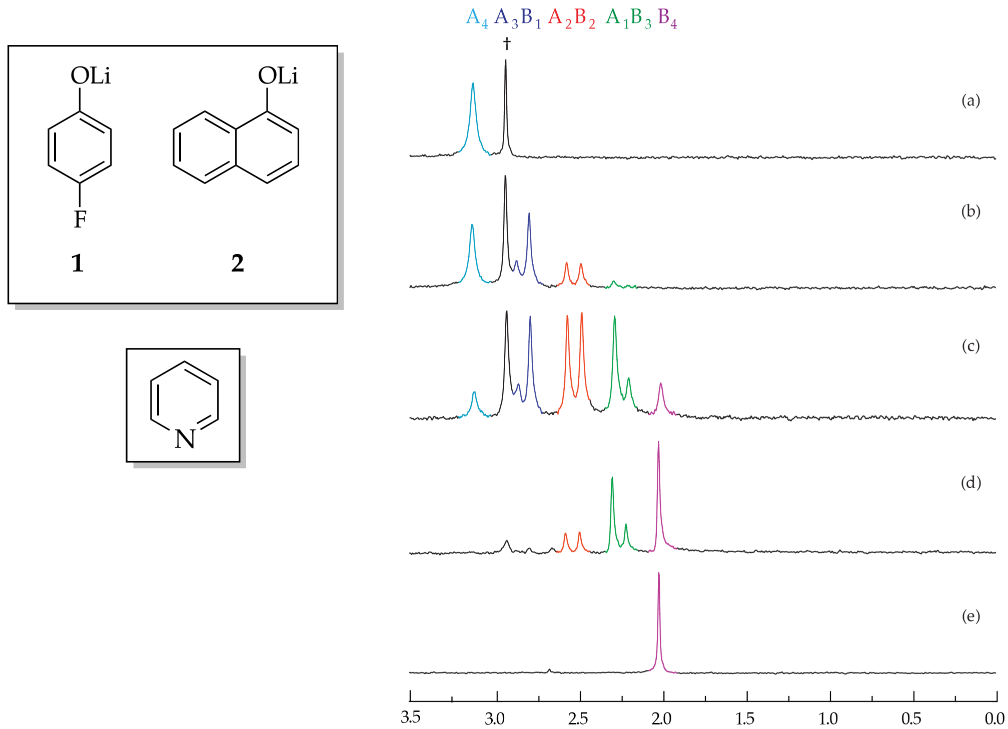

Figure 14. ^{6}Li NMR spectra of 0.10 M solutions of [^{6}Li]**2** (**A**) and [^{6}Li]**1** (**B**) in 0.50 M pyridine/toluene at -80 °C. The measured mole fractions of **A** in (a)-(e) are 1.00, 0.80, 0.50, 0.13, and 0.00, respectively. † indicates unknown aggregate.

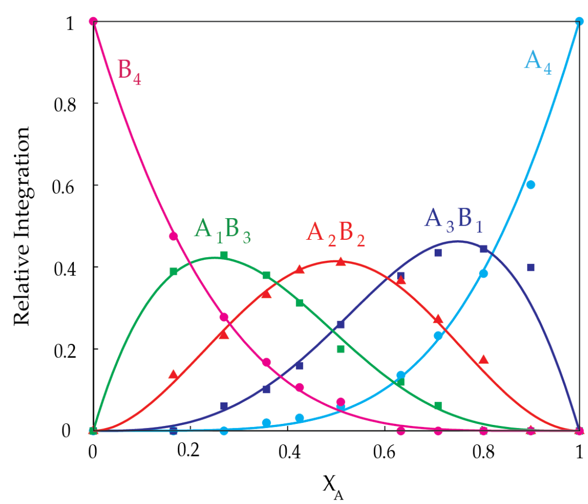

Figure 15. Job plot showing the relative integrations versus the measured mole fractions of **2** for 0.10 M mixtures of [^{6}Li]**2** (**A**) and [^{6}Li]**1** (**B**) in 0.50 M pyridine/toluene at -80 °C.

Tetramer Job Plots in Pyridine

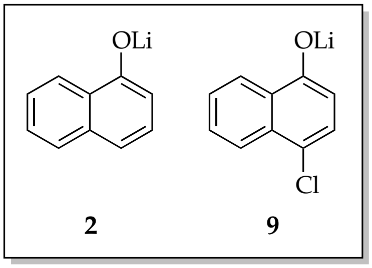

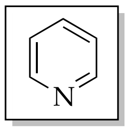

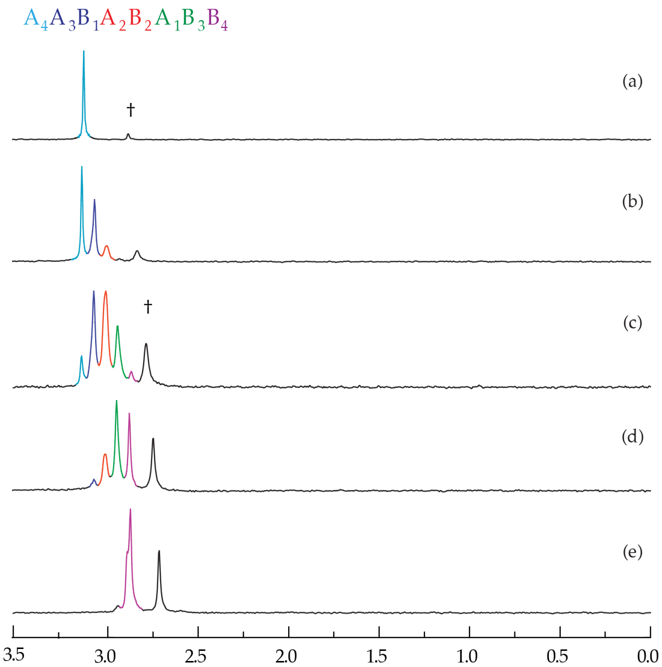

Figure 16. [6]Li NMR spectra of 0.10 M solutions of [[6]Li]**2** (**A**) and [[6]Li]**1** (**B**) in 0.50 M pyridine/toluene at -80 °C. The measured mole fractions of **A** in (a)-(e) are 1.00, 0.63, 0.49, 0.29, and 0.00, respectively. † indicates unknown aggregate.

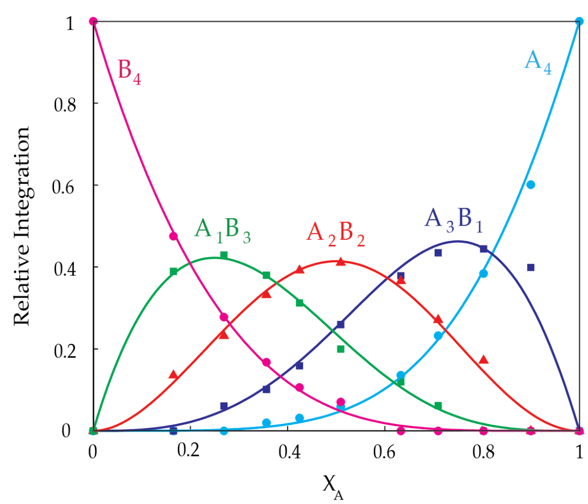

Figure 17. Job plot showing the relative integrations versus the measured mole fractions of **2** for 0.10 M mixtures of [[6]Li]**2** (**A**) and [[6]Li]**1** (**B**) in 0.50 M pyridine/toluene at -80 °C.

Dimer Job Plots in Pyridine

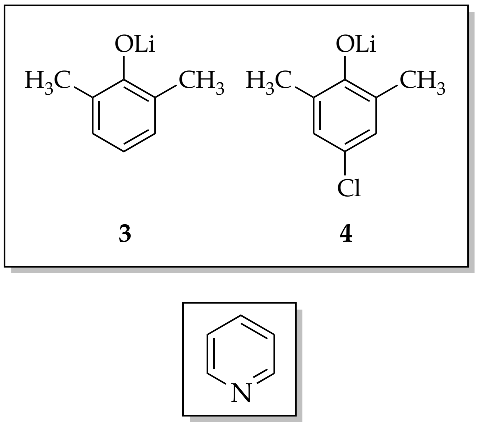

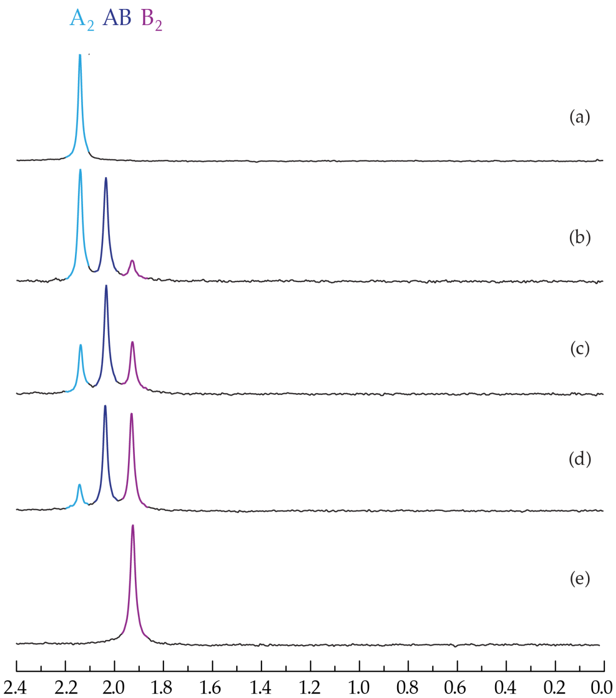

Figure 18. ^{6}Li NMR spectra of 0.10 M solutions of [^{6}Li]**3** (**A**) and [^{6}Li]**4** (**B**) in 0.50 M pyridine/toluene at -100 °C. The measured mole fractions of **A** in (a)-(e) are 1.00, 0.66, 0.56, 0.33, and 0.00, respectively.

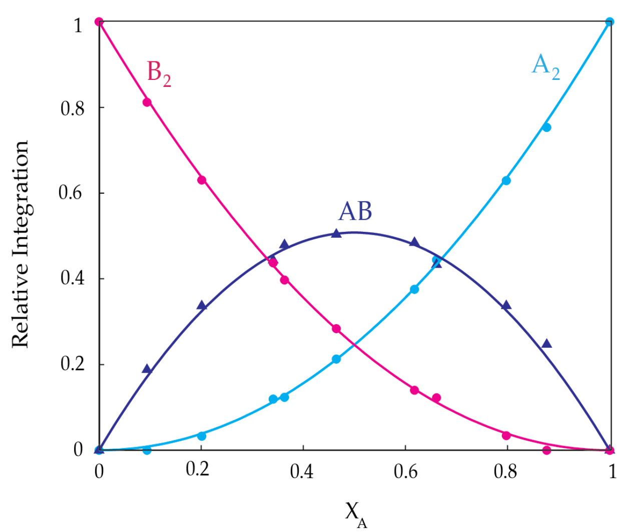

Figure 19. Job plot showing the relative integrations versus the measured mole fractions of **3** for 0.10 M mixtures of [^{6}Li]**3** (**A**) and [^{6}Li]**4** (**B**) in 0.50 M pyridine/toluene at -100 °C.

Tetramer Job Plots in Dimethylacetamide

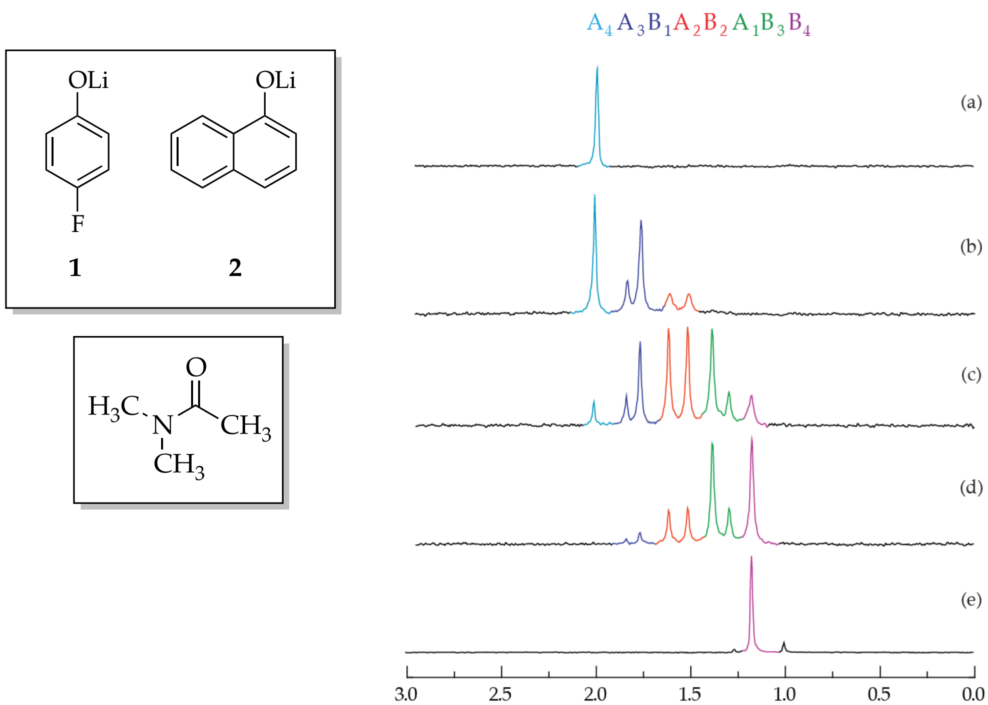

Figure 20. ^{6}Li NMR spectra of 0.10 M solutions of [^{6}Li]**2** (**A**) and [^{6}Li]**1** (**B**) in 0.50 M dimethylacetamide/toluene at -80 °C. The measured mole fractions of **A** in (a)-(e) are 1.00, 0.64, 0.45, 0.25, and 0.00, respectively.

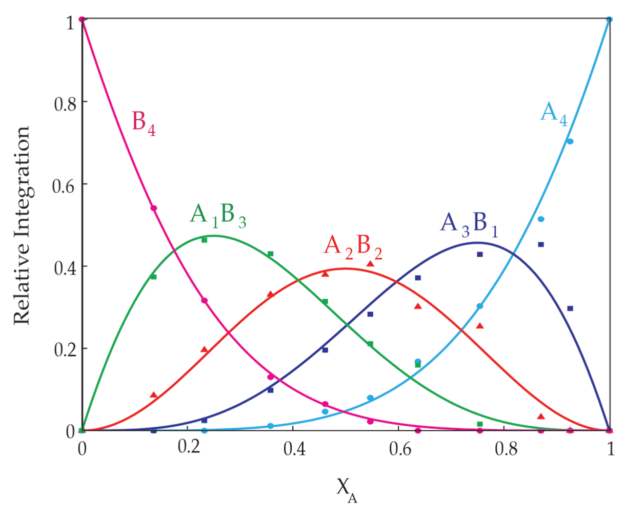

Figure 21. Job plot showing the relative integrations versus the measured mole fractions of **2** for 0.10 M mixtures of [^{6}Li]**2** (**A**) and [^{6}Li]**1** (**B**) in 0.50 M dimethylacetamide/toluene at -80 °C.

Tetramer Job Plots in Dimethylacetamide

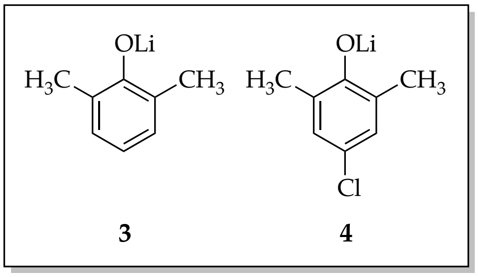

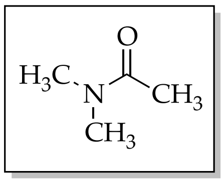

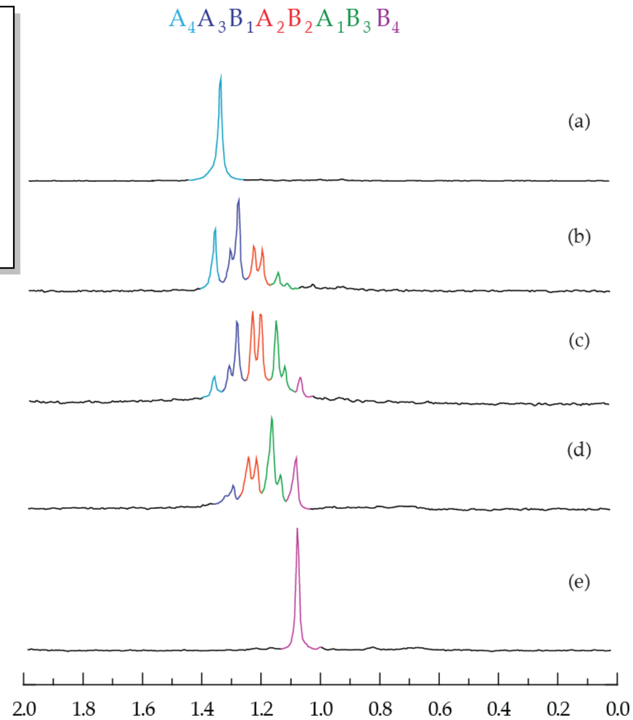

Figure 22. ^{6}Li NMR spectra of 0.10 M solutions of [^{6}Li]**3** (**A**) and [^{6}Li]**4** (**B**) in 0.50 M dimethylacetamide/toluene at -80 °C. The measured mole fractions of **A** in (a)-(e) are 1.00, 0.61, 0.50, 0.29, and 0.00, respectively.

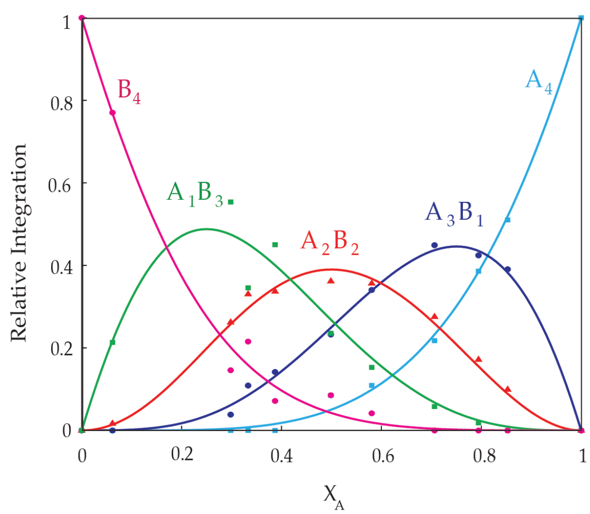

Figure 23. Job plot showing the relative integrations versus the measured mole fractions of **3** for 0.10 M mixtures of [^{6}Li]**3** (**A**) and [^{6}Li]**4** (**B**) in 0.50 M dimethylacetamide/toluene at -80 °C.

Tetramer Job Plots in Dimethylformamide

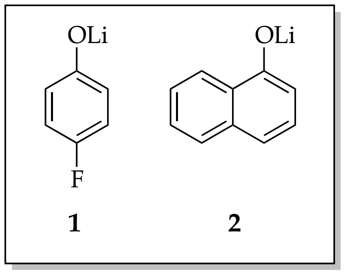

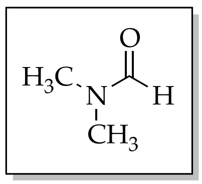

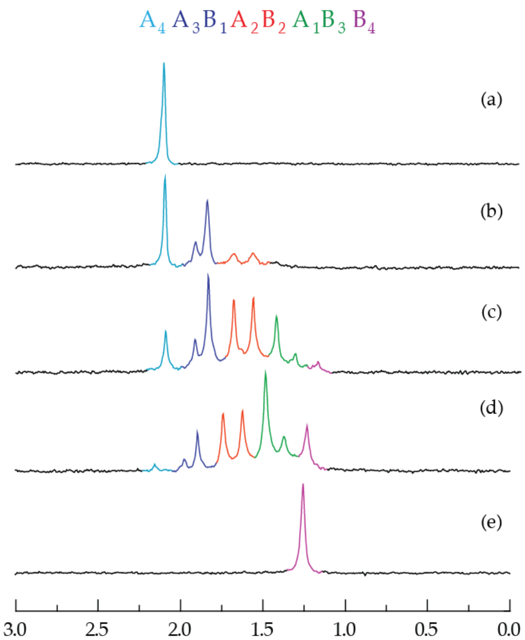

Figure 24. ^{6}Li NMR spectra of 0.10 M solutions of [^{6}Li]**2** (**A**) and [^{6}Li]**1** (**B**) in 0.50 M dimethylforamide/toluene at -80 °C. The measured mole fractions of **A** in (a)-(e) are 1.00, 0.65, 0.44, 0.23, and 0.00, respectively.

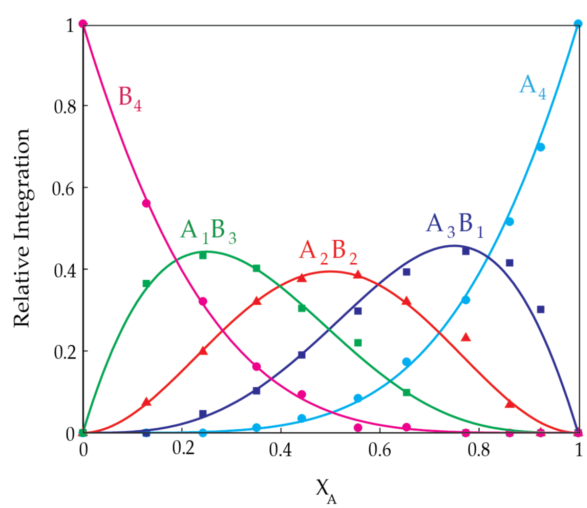

Figure 25. Job plot showing the relative integrations versus the measured mole fractions of **2** for 0.10 M mixtures of [^{6}Li]**2** (**A**) and [^{6}Li]**1** (**B**) in 0.50 M dimethylformamide/toluene at -80 °C.

Tetramer Job Plots in Dimethylsulfoxide

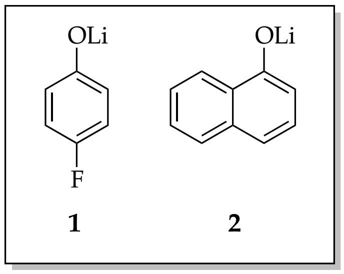

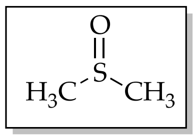

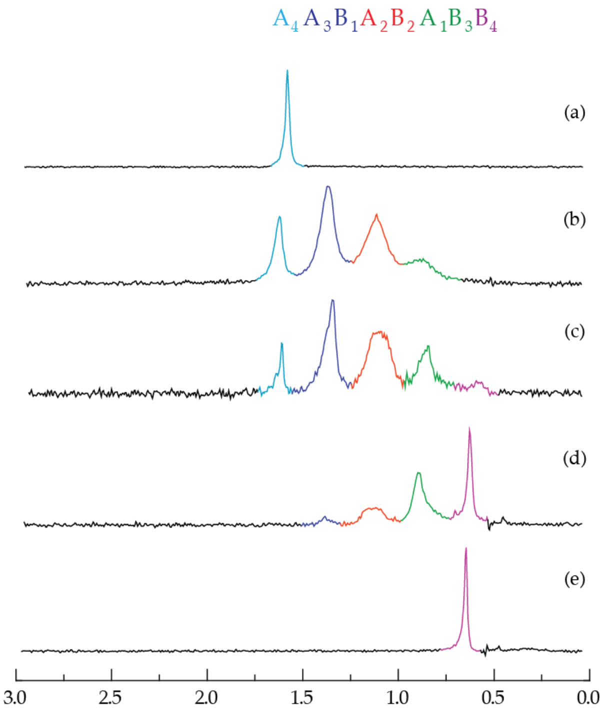

Figure 26. [6]Li NMR spectra of 0.10 M solutions of [[6]Li]**2** (**A**) and [[6]Li]**1** (**B**) in 0.50 M DMSO/toluene at -80 °C. The measured mole fractions of **A** in (a)-(e) are 1.00, 0.76, 0.46, 0.37, and 0.00, respectively.

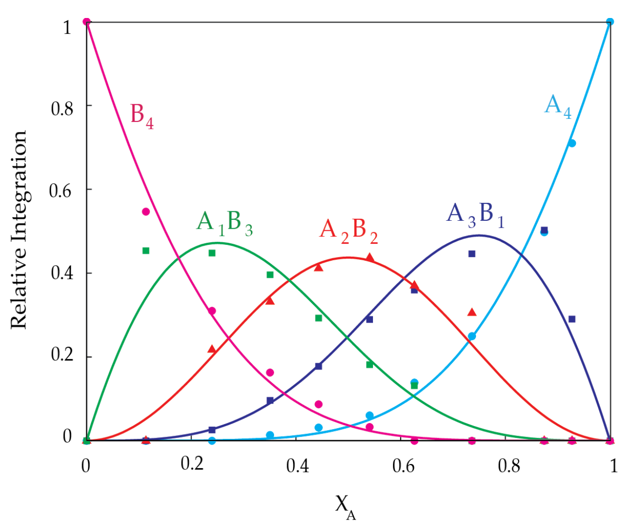

Figure 27. Job plot showing the relative integrations versus the measured mole fractions of **2** for 0.10 M mixtures of [[6]Li]**2** (**A**) and [[6]Li]**1** (**B**) in 0.50 M DMSO/toluene at -80 °C.

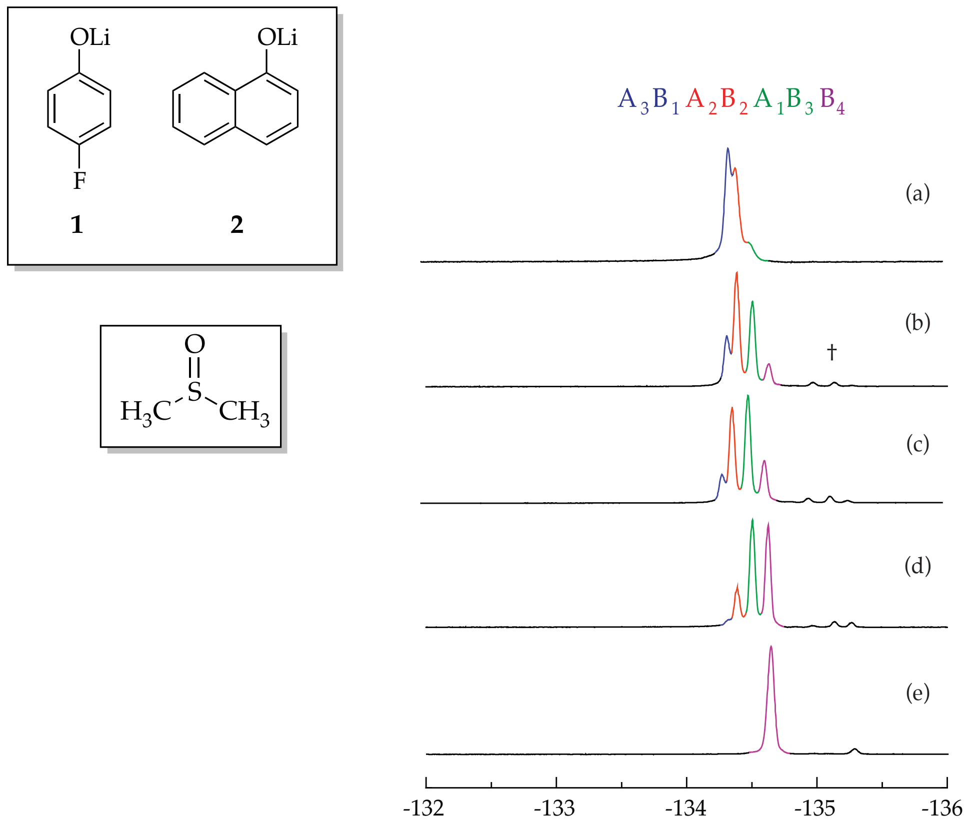

Figure 28. ^{19}F NMR spectra of 0.10 M solutions of [^{6}Li]**2** (**A**) and [^{6}Li]**1** (**B**) in 0.50 M dimethylsulfoxide/toluene at -80 °C. The mole fractions of **A** in (a)-(e) are roughly 0.90, 0.70, 0.40, 0.20, and 0.00, respectively.The naphtholate homoaggregate is invisible by ^{19}F NMR, so the A_3B_1 is the last observable species. At high naphtholate mole fraction, resolution becomes difficult and the A_2B_2 aggregate becomes a minor shoulder on the A_3B_1 peak. † appears to be a minor trimer component.

Trimer Job Plots in Dimethylsulfoxide

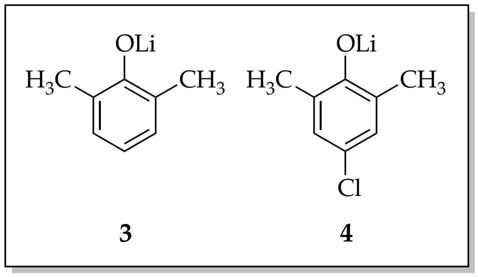

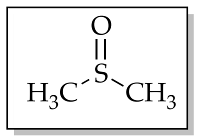

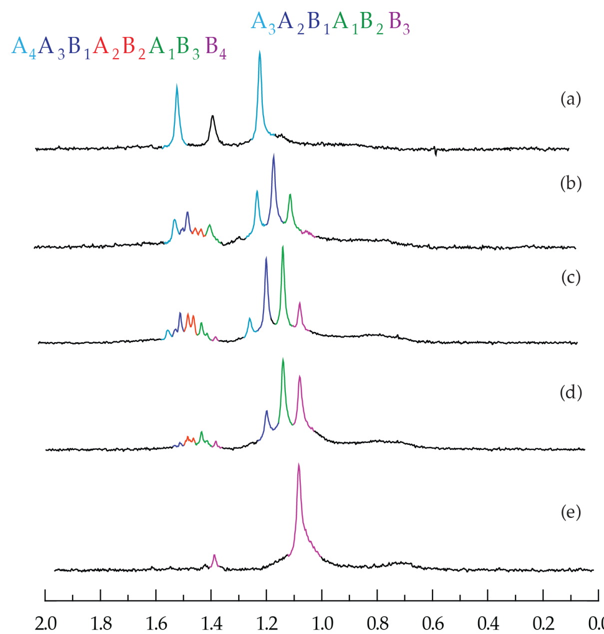

Figure 29. ^{6}Li NMR spectra of 0.10 M solutions of [^{6}Li]**3** (**A**) and [^{6}Li]**1** (**B**) in 0.50 M DMSO/toluene at -80 °C. The measured mole fractions of **A** in (a)-(e) are 1.00, 0.69, 0.54, 0.32, and 0.00, respectively.

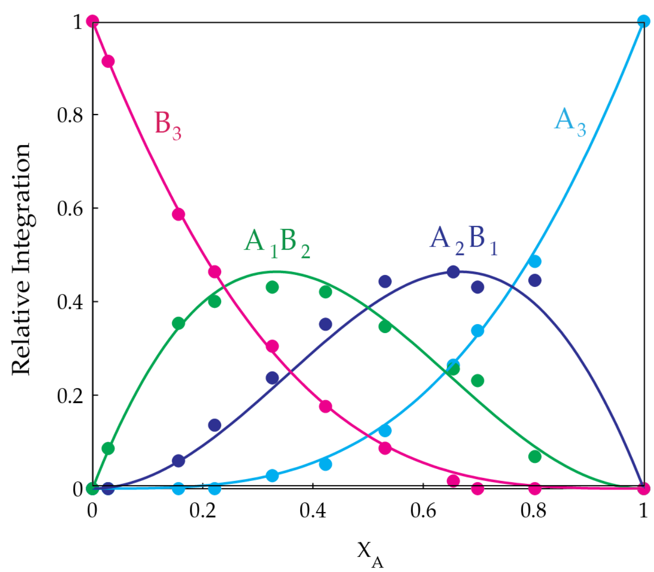

Figure 30. Job plot showing the relative integrations versus the measured mole fractions of **3** for 0.10 M mixtures of [^{6}Li]**3** (**A**) and [^{6}Li]**4** (**B**) in 0.50 M DMSO/toluene at -80 °C.

Tetramer Job Plots in DMPU

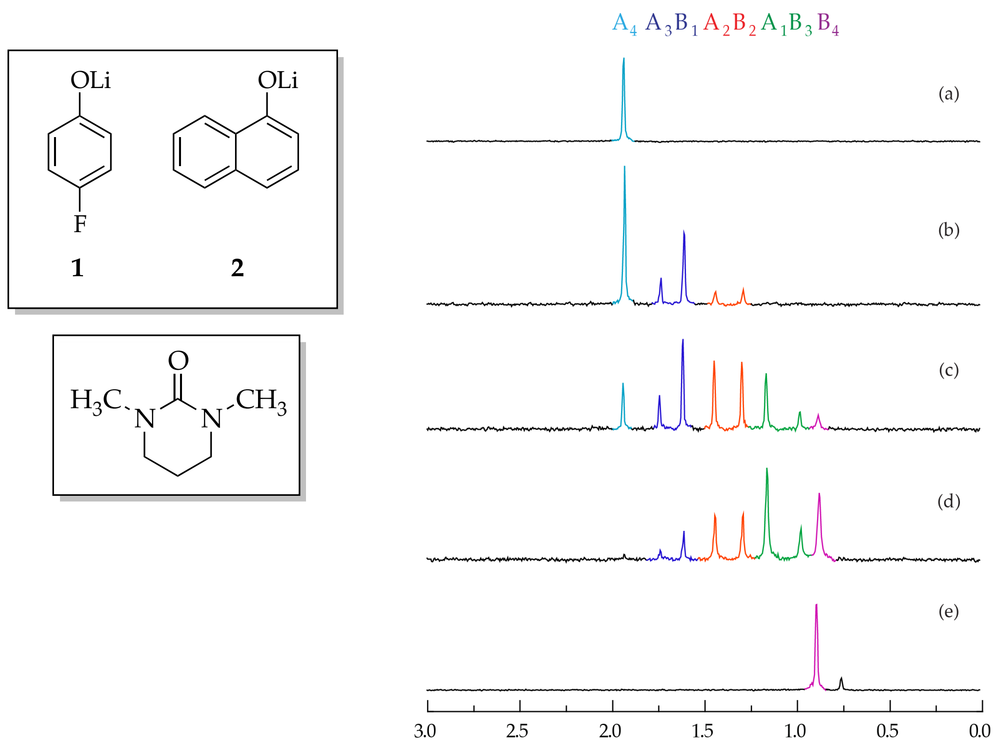

Figure 31. [6]Li NMR spectra of 0.10 M solutions of [[6]Li]**2** (**A**) and [[6]Li]**1** (**B**) in 0.50 M DMPU/toluene at -80 °C. The measured mole fractions of **A** in (a)-(e) are 1.00, 0.70, 0.46, 0.15, and 0.00, respectively.

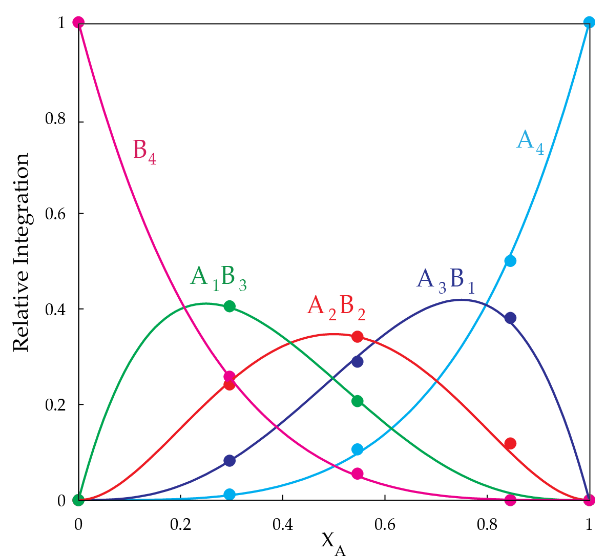

Figure 32. Job plot showing the relative integrations versus the measured mole fractions of **2** for 0.10 M mixtures of [[6]Li]**2** (**A**) and [[6]Li]**1** (**B**) in 0.50 M DMPU/toluene at -80 °C.

Tetramer Job Plots in DMPU

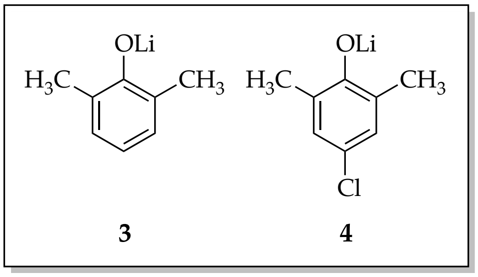

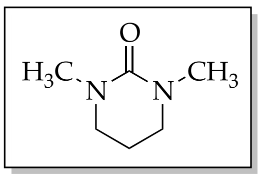

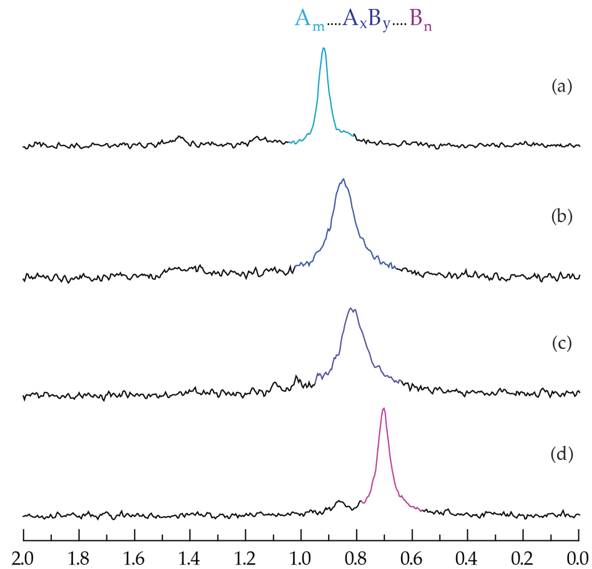

Figure 33. ^{6}Li NMR spectra of 0.10 M solutions of [^{6}Li]**3** (**A**) and [^{6}Li]**4** (**B**) in 0.50 M DMPU/toluene at -80 °C. The measured mole fractions cannot be calculated, but tubes (a) and (d) are **3** and **4,** respectively, whereas tubes (b) and (c) are mixtures.

Tetramer Job Plots in *N*-Methylpyrrolidone

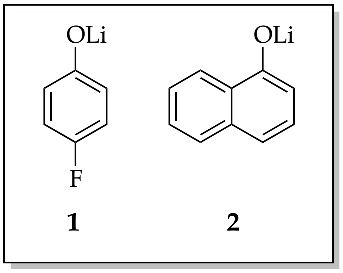

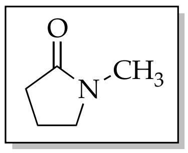

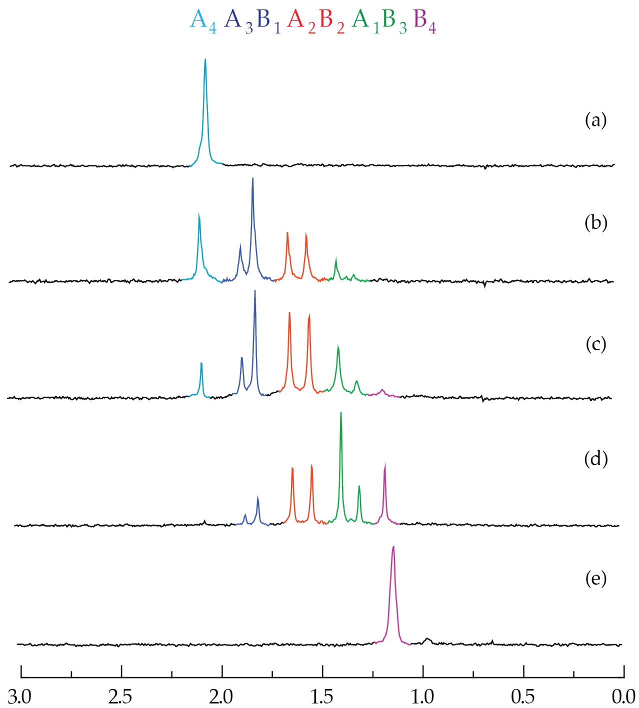

Figure 34. [6]Li NMR spectra of 0.10 M solutions of [[6]Li]**2** (**A**) and [[6]Li]**1** (**B**) in 0.50 M *N*-methylpyrrolidone/toluene at -85 °C. The measured mole fractions of **A** in (a)-(e) are 1.00, 0.65, 0.44, 0.30, and 0.00, respectively.

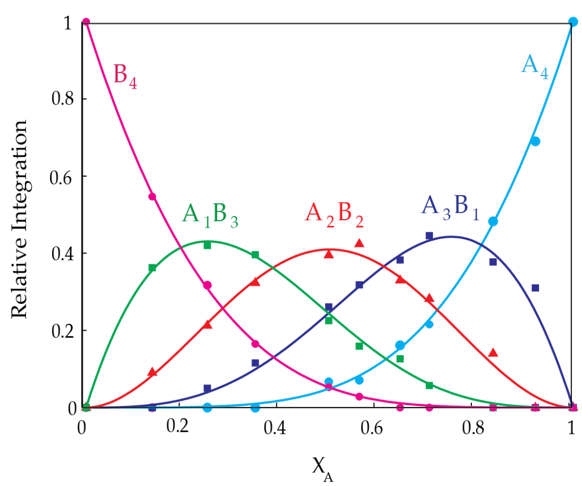

Figure 35. Job plot showing the relative integrations versus the measured mole fractions of **2** for 0.10 M mixtures of [[6]Li]**2** (**A**) and [[6]Li]**1** (**B**) in 0.50 M *N*-methylpyrrolidone/ toluene at -85 °C.

Tetramer Job Plots in *N*-Methylpyrrolidone

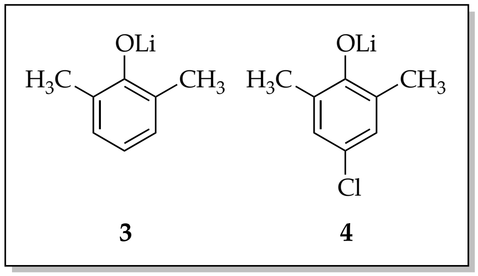

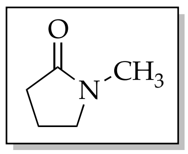

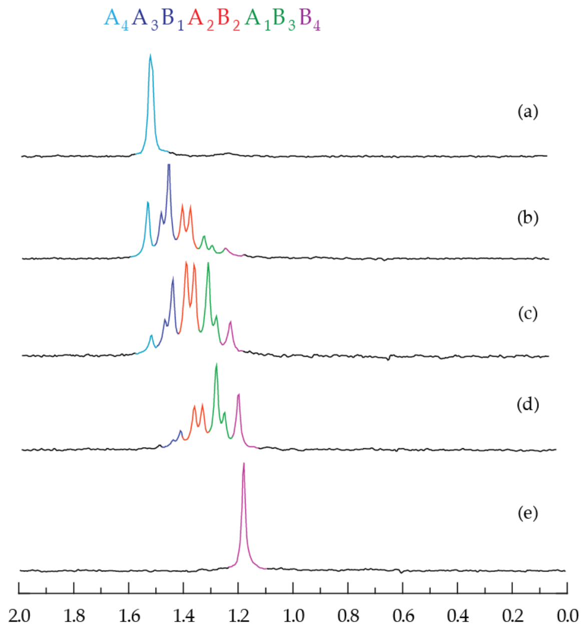

Figure 36. ⁶Li NMR spectra of 0.10 M solutions of [⁶Li]**3** (**A**) and [⁶Li]**4** (**B**) in 0.50 M *N*-methylpyrrolidone/toluene at -80 °C. The measured mole fractions of **A** in (a)-(e) are 1.00, 0.68, 0.53, 0.33, and 0.00, respectively.

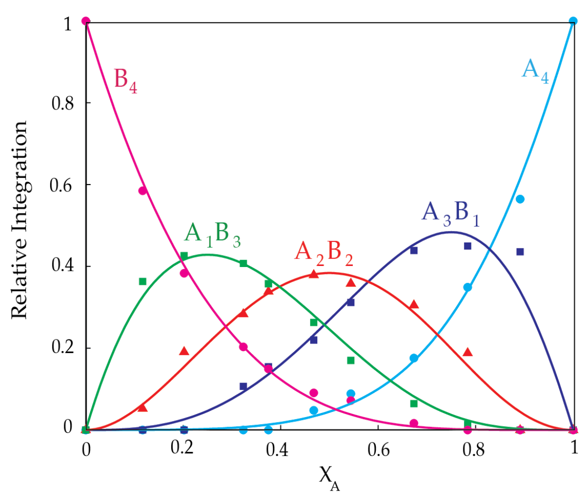

Figure 37. Job plot showing the relative integrations versus the measured mole fractions of **3** for 0.10 M mixtures of [⁶Li]**3** (**A**) and [⁶Li]**4** (**B**) in 0.50 M *N*-methylpyrrolidone/toluene at -80 °C.

<u>**Tetramer Job Plots in *n*-Propylamine**</u>

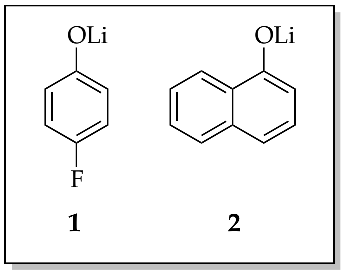

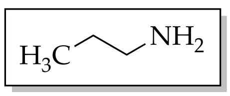

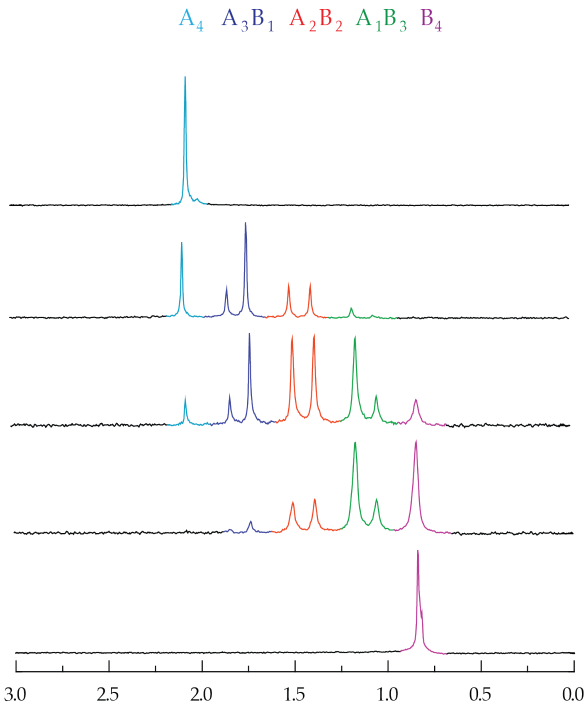

Figure 38. ^{6}Li NMR spectra of 0.10 M solutions of [^{6}Li]**2** (**A**) and [^{6}Li]**1** (**B**) in 0.50 M *n*-PrNH$_2$/toluene at -80 °C. The measured mole fractions of **A** in (a)-(e) are 1.00, 0.76, 0.56, 0.28, and 0.00, respectively.

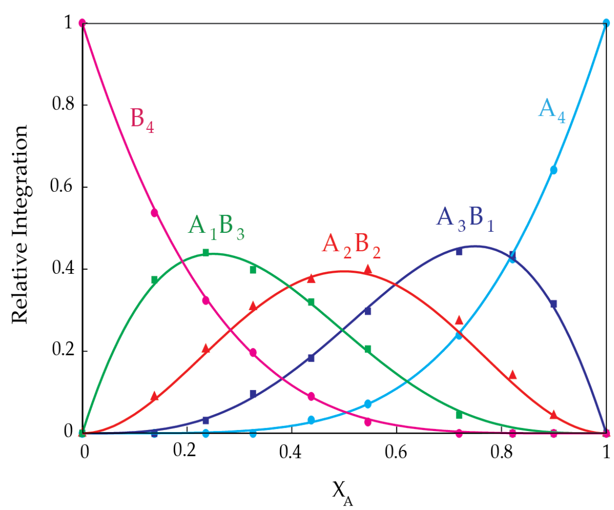

Figure 39. Job plot showing the relative integrations versus the measured mole fractions of **2** for 0.10 M mixtures of [^{6}Li]**2** (**A**) and [^{6}Li]**1** (**B**) in 0.50 M *n*-PrNH$_2$/toluene at -80 °C.

Dimer Job Plots in *n*-Propylamine

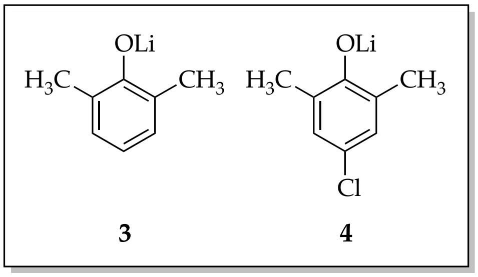

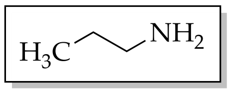

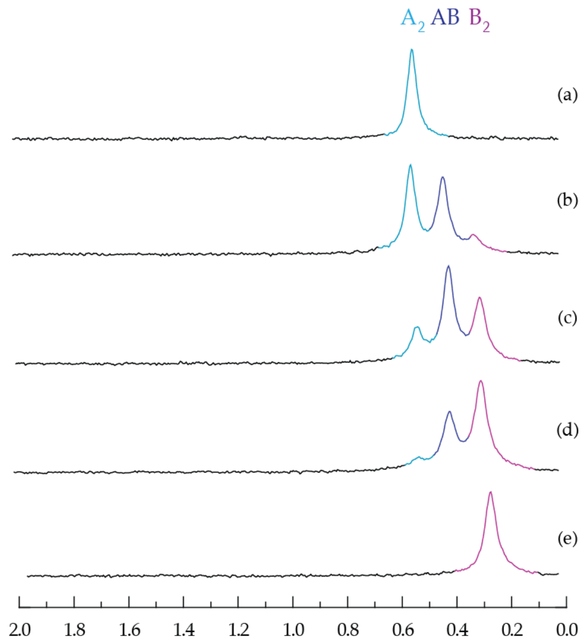

Figure 40. ^{6}Li NMR spectra of 0.10 M solutions of [^{6}Li]**3** (**A**) and [^{6}Li]**4** (**B**) in 0.50 M *n*-PrNH$_2$/toluene at -110 °C. The measured mole fractions of **A** in (a)-(e) are 1.00, 0.73, 0.58, 0.34, and 0.00, respectively.

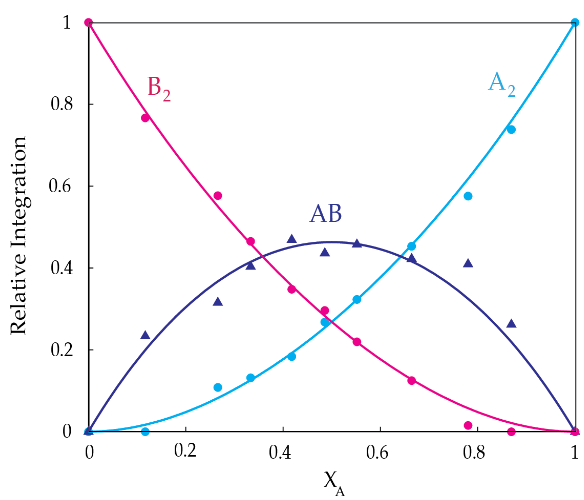

Figure 41. Job plot showing the relative integrations versus the measured mole fractions of **3** for 0.10 M mixtures of [^{6}Li]**3** (**A**) and [^{6}Li]**4** (**B**) in 0.50 M *n*-PrNH$_2$/toluene at -110 °C.

Tetramer Job Plots in Piperidine

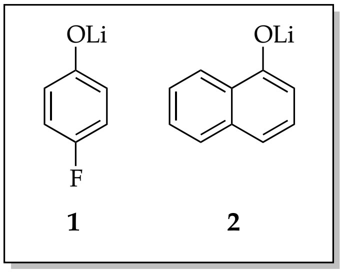

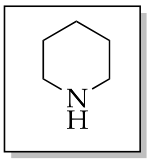

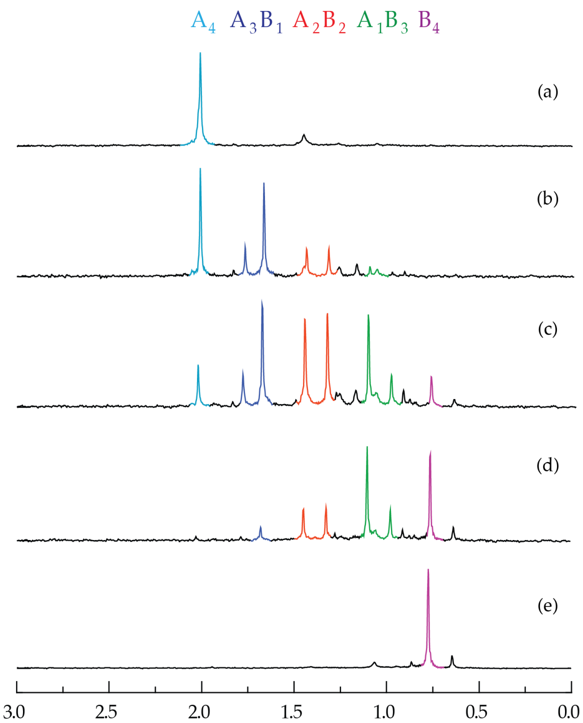

Figure 42. ^{6}Li NMR spectra of 0.10 M solutions of [^{6}Li]**2** (**A**) and [^{6}Li]**1** (**B**) in 0.50 M piperidine/toluene at -60 °C. The measured mole fractions of **A** in (a)-(e) are 1.00, 0.74, 0.48, 0.21, and 0.00, respectively.

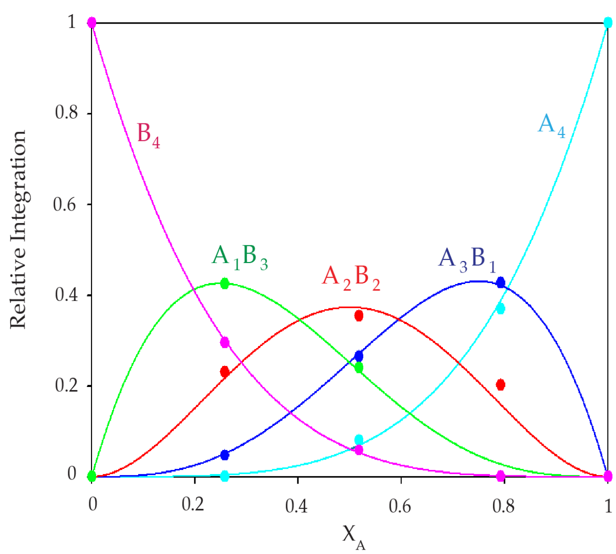

Figure 43. Job plot showing the relative integrations versus the measured mole fractions of **2** for 0.10 M mixtures of [^{6}Li]**2** (**A**) and [^{6}Li]**1** (**B**) in 0.50 M piperidine/toluene at -60 °C.

^{19}F Spectra in Piperidine

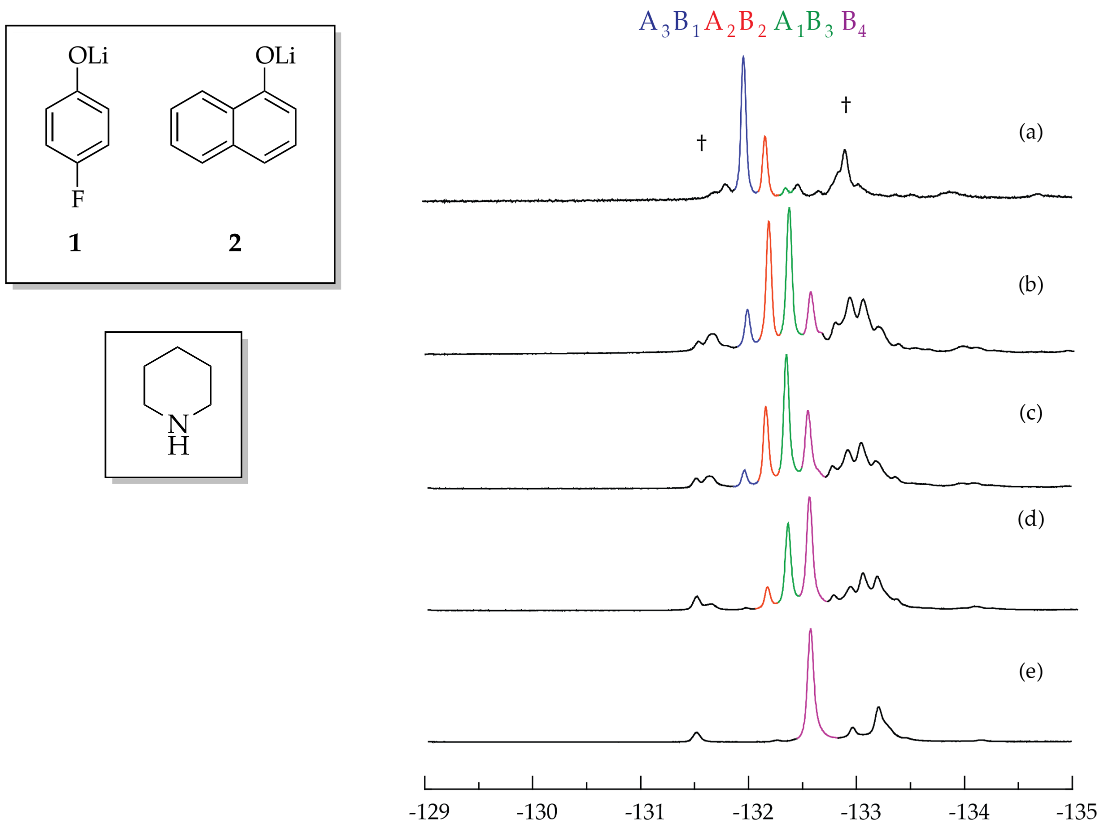

Figure 44. ^{19}F NMR spectra of 0.10 M solutions of [^{6}Li]**2** (**A**) and [^{6}Li]**1** (**B**) in 0.50 M piperidine/toluene at -80 °C. The mole fractions of **A** in (a)-(e) are roughly 0.90, 0.60, 0.40, 0.20, and 0.00, respectively.The naphtholate homoaggregate is invisible by ^{19}F NMR, so the A_3B_1 is the last observable species. **1** has three additional resonances, which form the unidentifiable ensembles denoted by †.

Trimer Job Plots in Piperidine

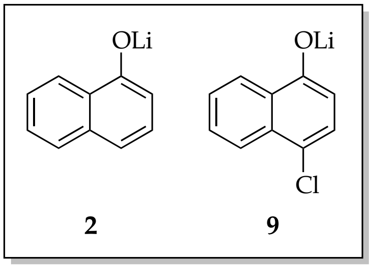

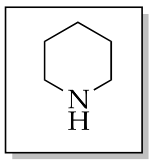

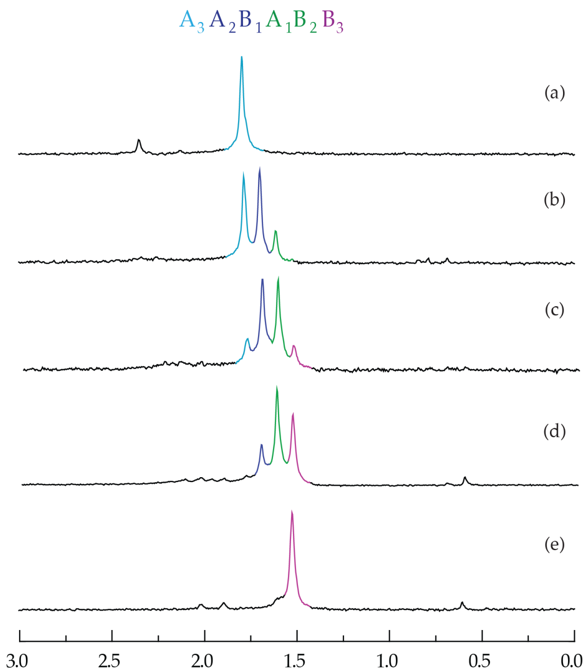

Figure 45. ^{6}Li NMR spectra of 0.10 M solutions of [^{6}Li]**2** (**A**) and [^{6}Li]**9** (**B**) in 0.50 M piperidine/toluene at -90 °C. The measured mole fractions of **A** in (a)-(e) are 1.00, 0.64, 0.43, 0.24, and 0.00, respectively.

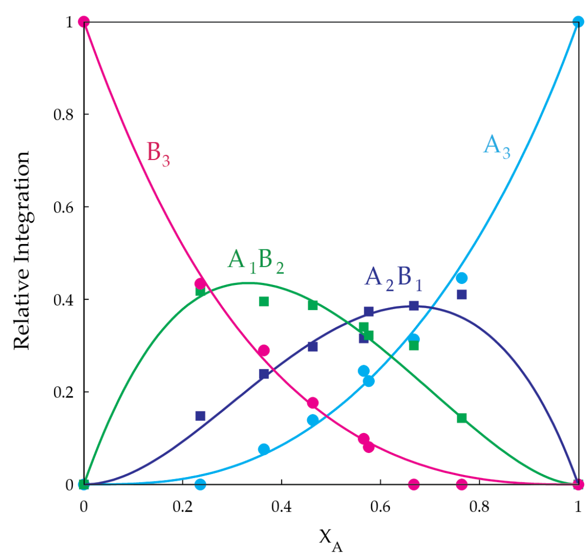

Figure 46. Job plot showing the relative integrations versus the measured mole fractions of **2** for 0.10 M mixtures of [^{6}Li]**2** (**A**) and [^{6}Li]**9** (**A**) in 0.50 M piperidine/toluene at -90 °C.

Job Plots in Piperidine

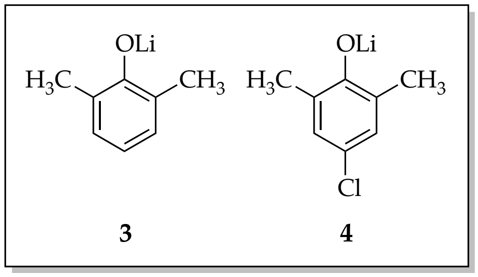

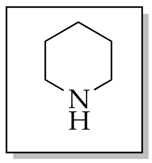

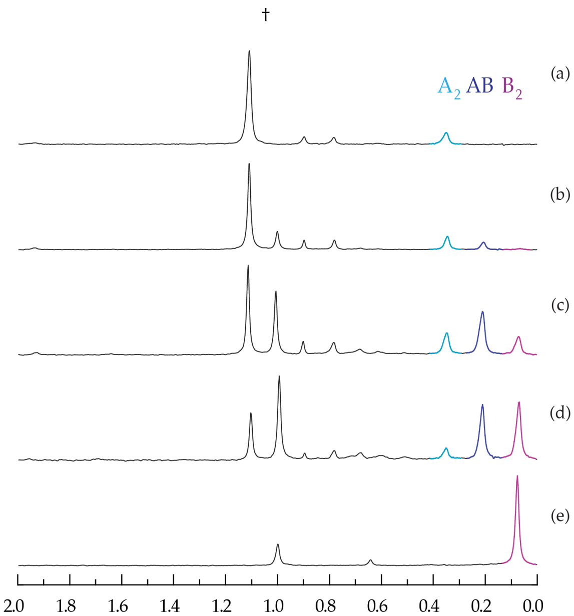

Figure 47. ^{6}Li NMR spectra of 0.10 M solutions of [^{6}Li]**2** (**A**) and [^{6}Li]**9** (**B**) in 0.50 M piperidine/toluene at -90 °C. The measured mole fractions of **A** in (a)-(e) are 1.00, 0.78, 0.52, 0.33, and 0.00, respectively. † indicates unknown aggregate.

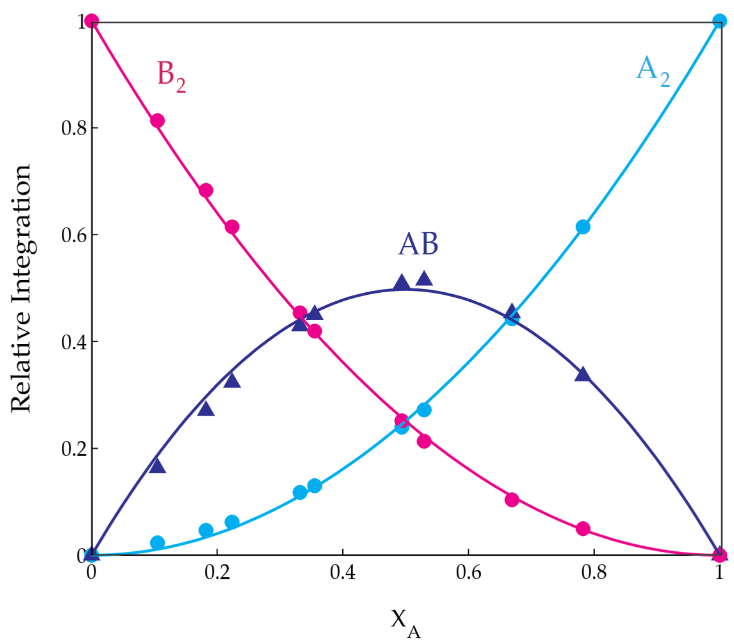

Figure 48. Job plot showing the relative integrations versus the measured mole fractions of **2** for 0.10 M mixtures of [^{6}Li]**2** (**A**) and [^{6}Li]**1** (**B**) in 0.50 M piperidine/toluene at -90 °C.

Job Plots in Pyrrolidine

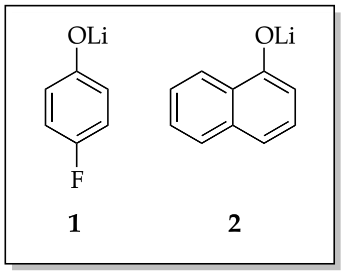

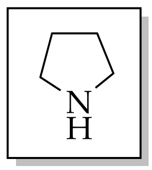

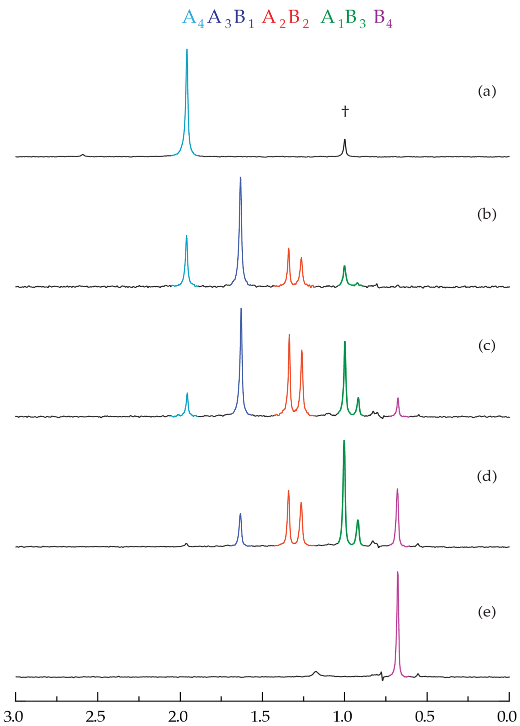

Figure 49. [6]Li NMR spectra of 0.10 M solutions of [[6]Li]**2** (**A**) and [[6]Li]**9** (**B**) in 0.50 M pyrrolidine/toluene at -90 °C. The measured mole fractions of **A** in (a)-(e) are 1.00, 0.69, 0.52, 0.35, and 0.00, respectively. † indicates unknown aggregate.

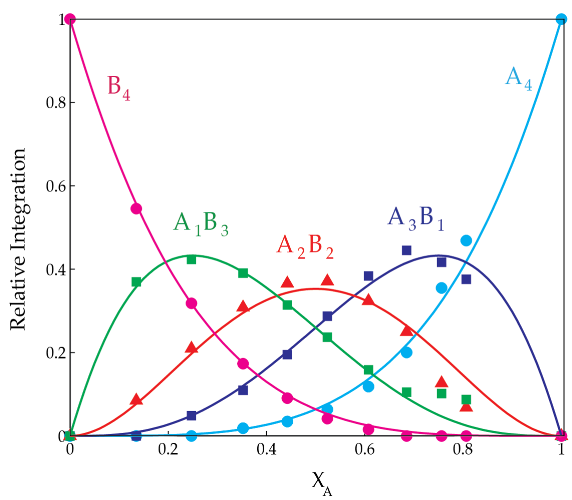

Figure 50. Job plot showing the relative integrations versus the measured mole fractions of **2** for 0.10 M mixtures of [[6]Li]**2** (**A**) and [[6]Li]**1** (**B**) in 0.50 M pyrrolidine/toluene at -90 °C.

Job Plots in Pyrrolidine

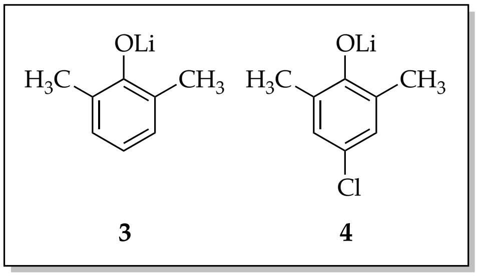

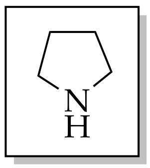

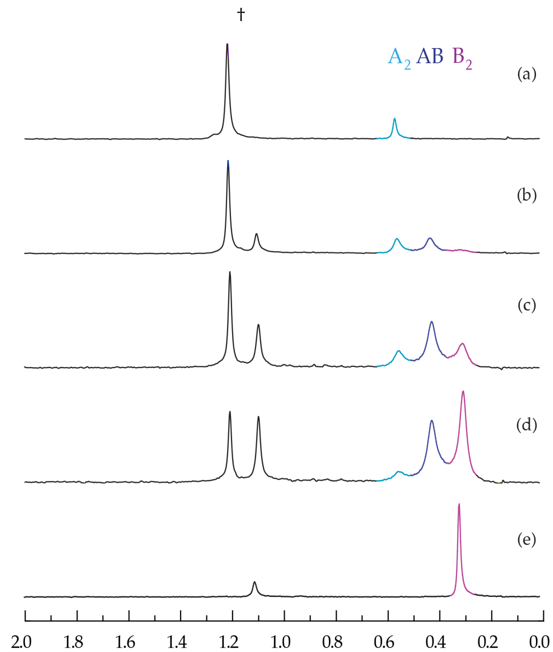

Figure 51. [6]Li NMR spectra of 0.10 M solutions of [[6]Li]**2** (**A**) and [[6]Li]**9** (**B**) in 0.50 M pyrrolidine/toluene at -90 °C. The measured mole fractions of **A** in (a)-(e) are 1.00, 0.58, 0.45, 0.29, and 0.00, respectively. † indicates unknown aggregate.

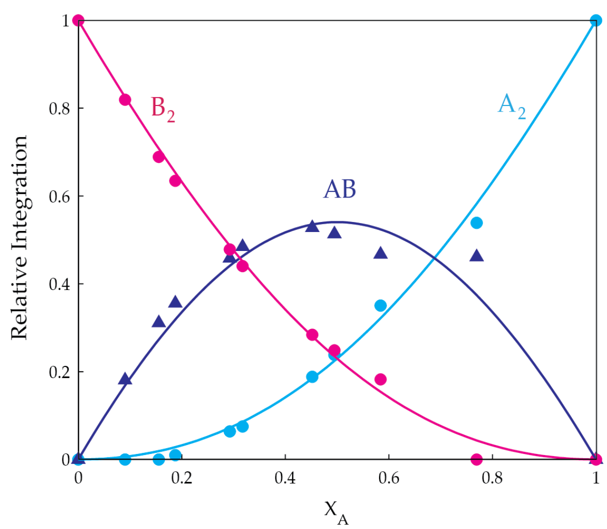

Figure 52. Job plot showing the relative integrations versus the measured mole fractions of **2** for 0.10 M mixtures of [[6]Li]**2** (**A**) and [[6]Li]**1** (**B**) in 0.50 M pyrrolidine/toluene at -90 °C.

<u>**Tetramer Job Plots in *i*-Butylamine**</u>

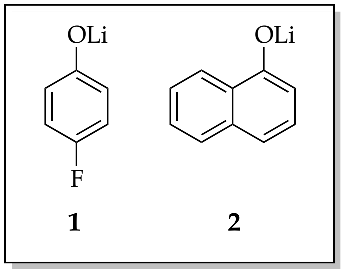

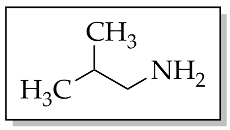

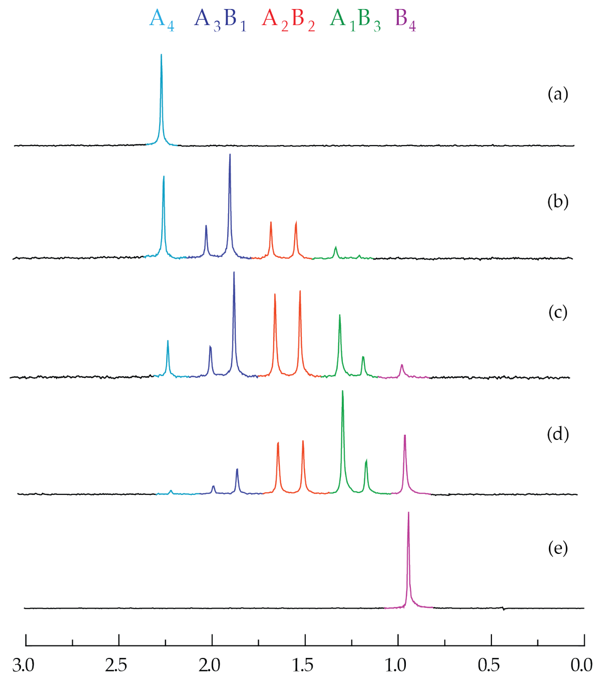

Figure 53. [6]Li NMR spectra of 0.10 M solutions of [[6]Li]**2** (**A**) and [[6]Li]**1** (**B**) in 0.50 M *i*-$BuNH_2$/toluene at -80 °C. The measured mole fractions of **A** in (a)-(e) are 1.00, 0.66, 0.53, 0.73, and 1.00, respectively.

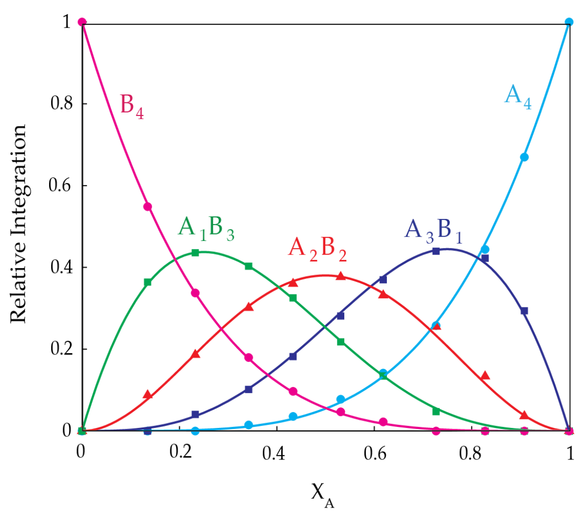

Figure 54. Job plot showing the relative integrations versus the measured mole fractions of **2** for 0.10 M mixtures of [[6]Li]**2** (**A**) and [[6]Li]**1** (**B**) in 0.50 M *i*-$BuNH_2$/toluene at -80 °C.

<u>**Dimer Job Plots in *i*-Butylamine**</u>

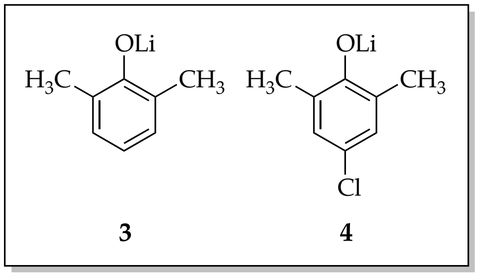

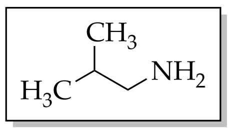

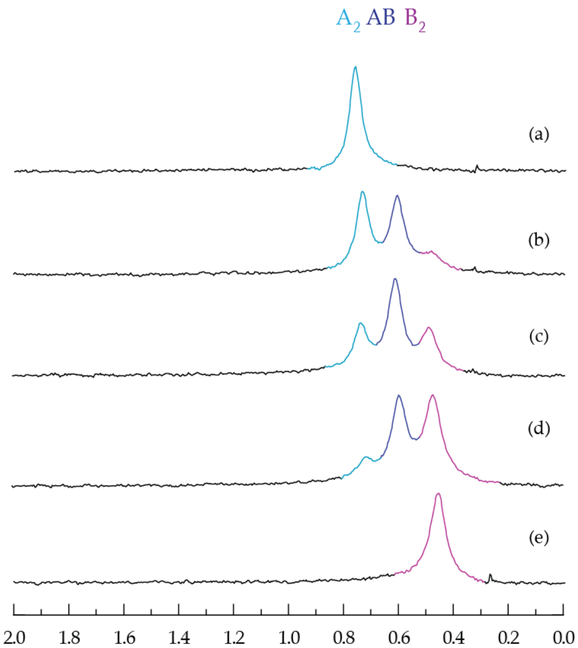

Figure 55. ^{6}Li NMR spectra of 0.10 M solutions of [^{6}Li]**3** (**A**) and [^{6}Li]**4** (**B**) in 0.50 M *i*-BuNH$_2$/toluene at -110 °C. The measured mole fractions of **A** in (a)-(e) are 1.00, 0.62, 0.48, 0.46, and 0.00, respectively.

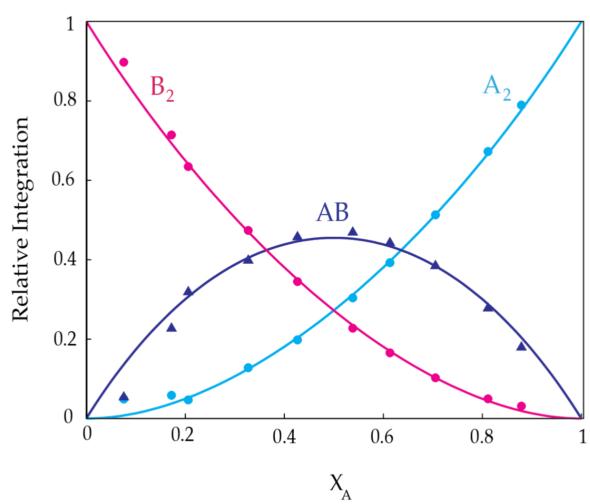

Figure 56. Job plot showing the relative integrations versus the measured mole fractions of **3** for 0.10 M mixtures of [^{6}Li]**3** (**A**) and [^{6}Li]**4** (**B**) in 0.50 M *i*-BuNH$_2$/toluene at -110 °C.

<u>**Tetramer Job Plots in *sec*-Butylamine**</u>

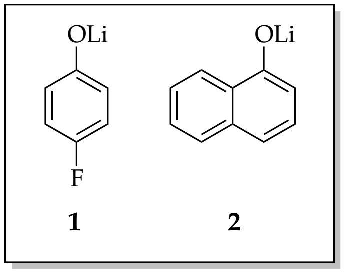

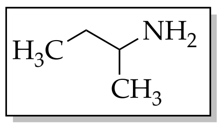

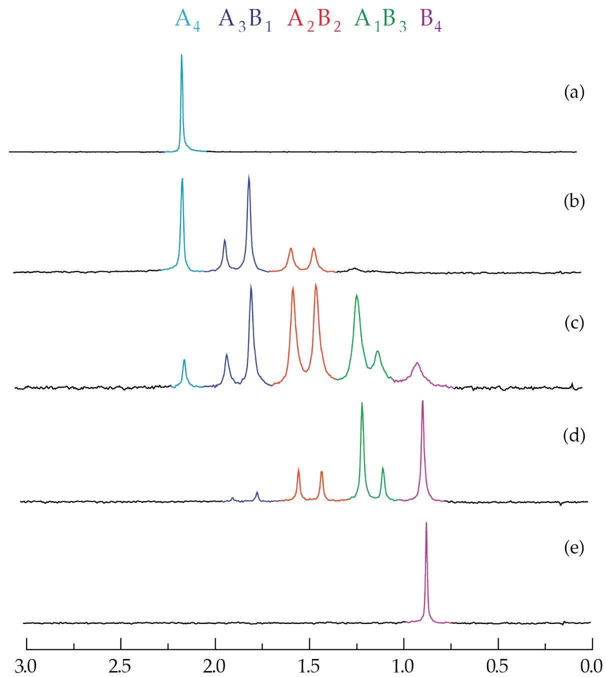

Figure 57. [6]Li NMR spectra of 0.10 M solutions of [[6]Li]**2** (**A**) and [[6]Li]**1** (**B**) in 0.50 M *sec*-BuNH$_2$/toluene at -60 °C. The measured mole fractions of **A** in (a)-(e) are 1.00, 0.76, 0.43, 0.28, and 1.00, respectively.

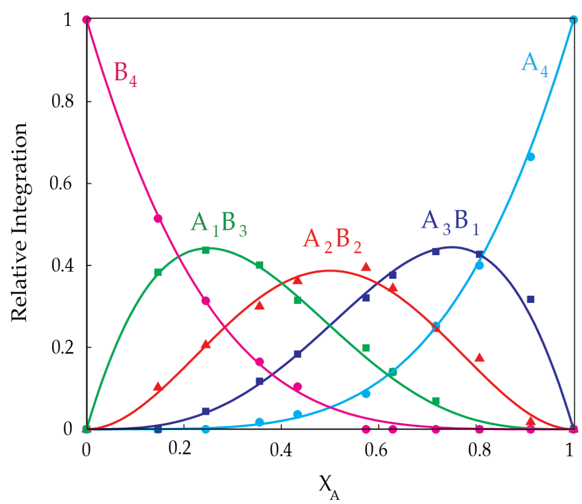

Figure 58. Job plot showing the relative integrations versus the measured mole fractions of **2** for 0.10 M mixtures of [[6]Li]**2** (**A**) and [[6]Li]**1** (**B**) in 0.50 M *sec*-BuNH$_2$/toluene at -60 °C.

<u>**Tetramer Job Plots in *t*-Butylamine**</u>

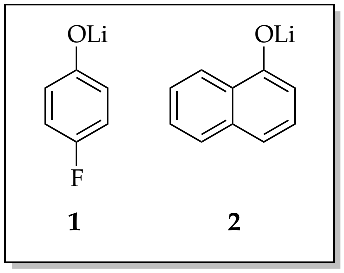

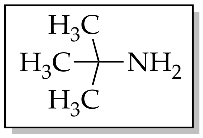

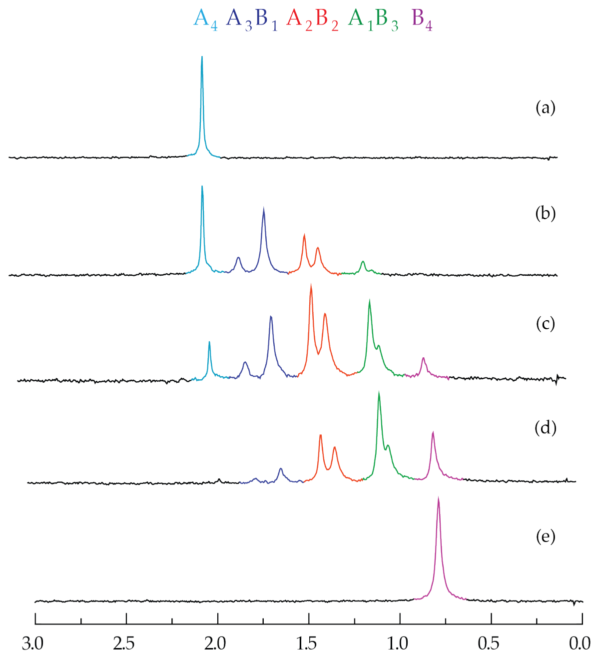

Figure 59. ^{6}Li NMR spectra of 0.10 M solutions of [^{6}Li]**2** (**A**) and [^{6}Li]**1** (**B**) in 0.50 M *t*-BuNH$_2$/toluene at -80 °C. The measured mole fractions of **A** in (a)-(e) are 1.00, 0.68, 0.53, 0.32, and 1.00, respectively.

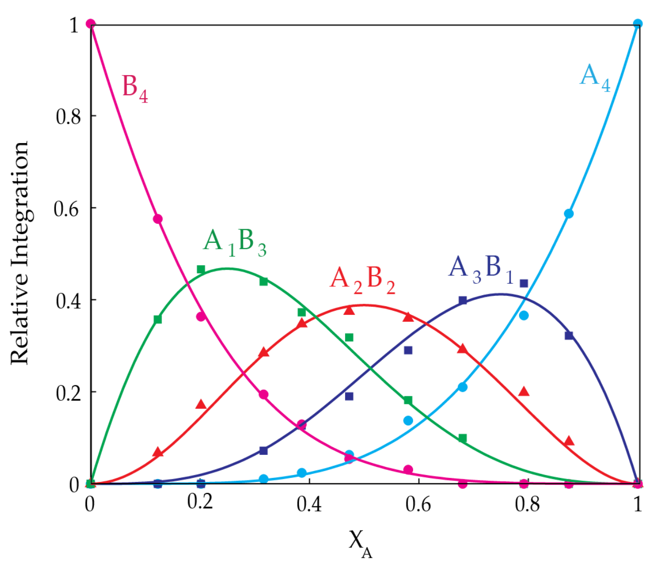

Figure 60. Job plot showing the relative integrations versus the measured mole fractions of **2** for 0.10 M mixtures of [^{6}Li]**2** (**A**) and [^{6}Li]**1** (**B**) in 0.50 M *t*-BuNH$_2$/toluene at -80 °C.

Trimer Job Plots in Diisopropylamine

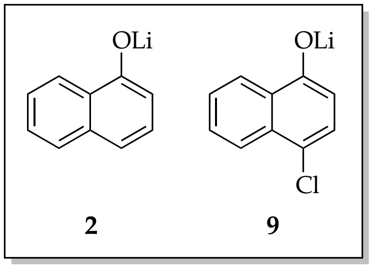

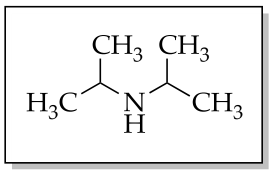

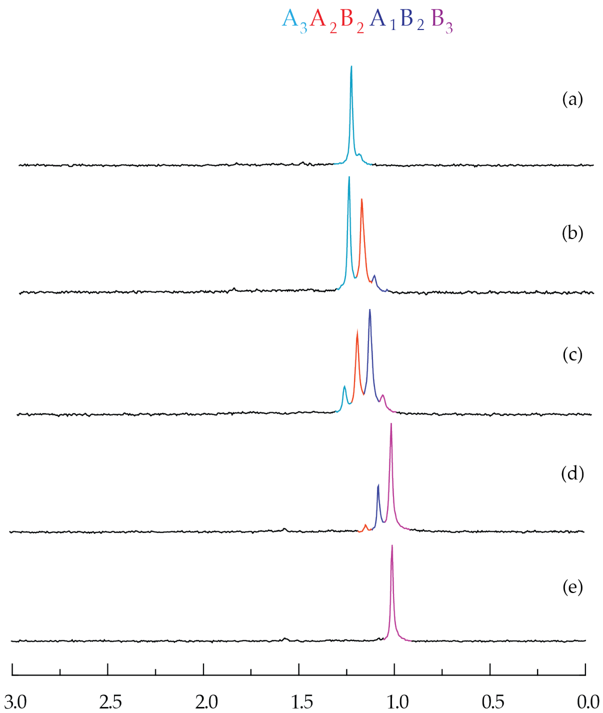

Figure 61. [6]Li NMR spectra of 0.10 M solutions of [[6]Li]**2** (**A**) and [[6]Li]**9** (**B**) in 1.0 M *i*-Pr_2NH/toluene at -60 °C. The measured mole fractions of **A** in (a)-(e) are 1.00, 0.89, 0.53, 0.23, and 0.00, respectively.

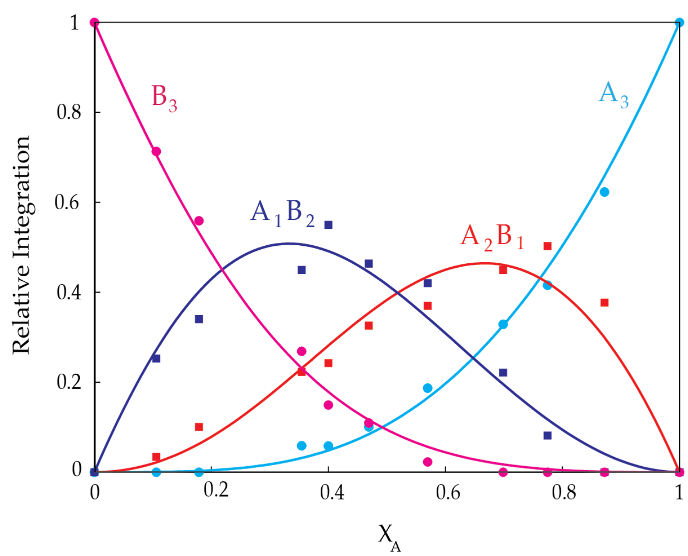

Figure 62. Job plot showing the relative integrations versus the measured mole fractions of **2** for 0.10 M mixtures of [[6]Li]**2** (**A**) and [[6]Li]**9** (**B**) in 1.0 M *i*-Pr_2NH/toluene at -60 °C.

^{6}Li Spectra in Diisopropylamine

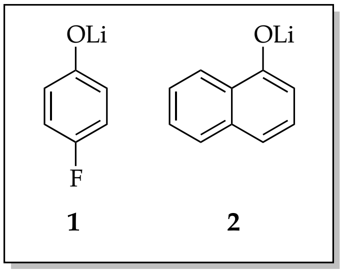

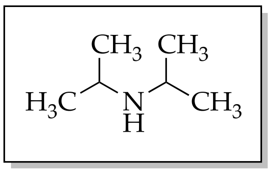

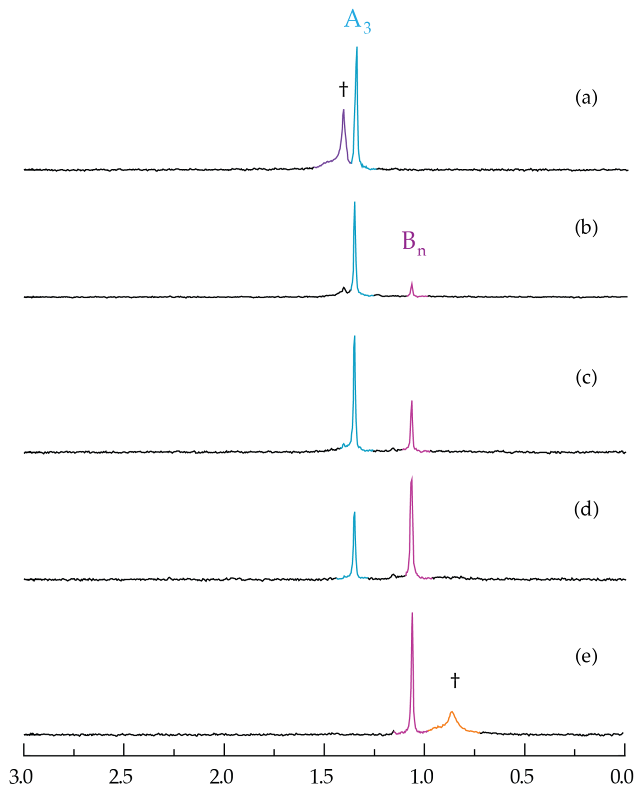

Figure 63. ^{6}Li NMR spectra of 0.10 M solutions of [^{6}Li]**2** (**A**) and [^{6}Li]**1** (**B**) in 1.0 M diisopropylamine/toluene at -40 °C. The mole fractions of **2** in (a)-(e) are approximately 1.00, 0.75, 0.50, 0.25, 0.00, respectively. The absence of heteroaggregate formation indicates that **2** and **1** are not the same aggregation state. **2** was characterized as a trimer (previous page). † indicates unknown aggregate.

<u>**Dimer Job Plots in Diisopropylamine**</u>

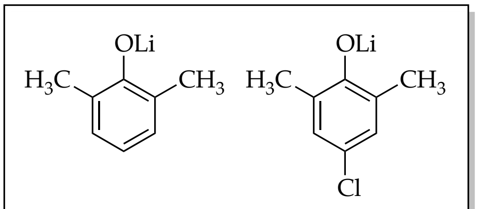

3 **4**

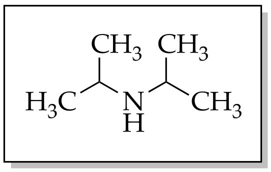

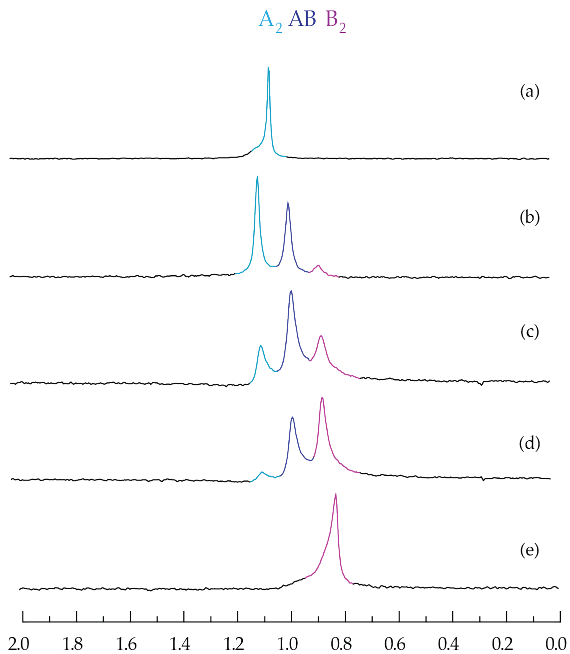

Figure 64. ^{6}Li NMR spectra of 0.10 M solutions of [^{6}Li]**3** (**A**) and [^{6}Li]**4** (**B**) in 1.0 M *i*-Pr_2NH/toluene at -80 °C. The measured mole fractions of **A** in (a)-(e) are 1.00, 0.73, 0.54, 0.31, and 0.00, respectively.

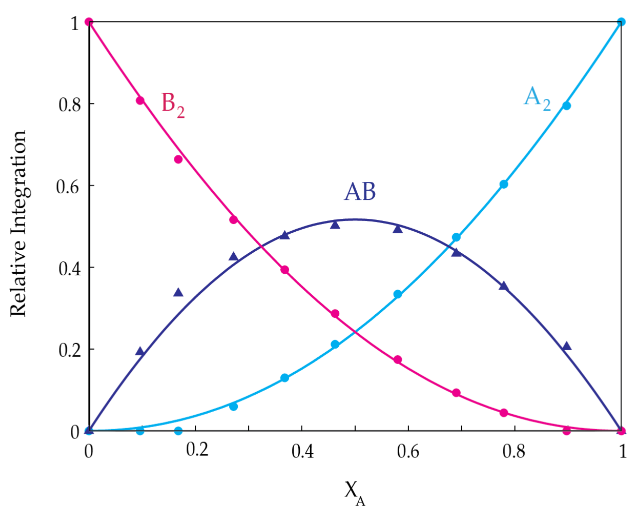

Figure 65. Job plot showing the relative integrations versus the measured mole fractions of **3** for 0.10 M mixtures of [^{6}Li]**3** (**A**) and [^{6}Li]**4** (**B**) in 1.0 M *i*-Pr_2NH/toluene at -80 °C.

Tetramer Job Plots in Diethylamine

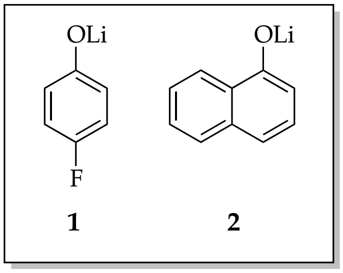

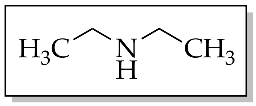

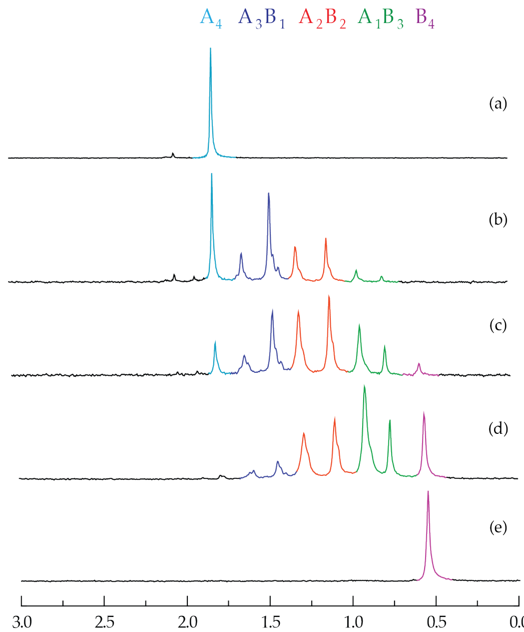

Figure 66. ^{6}Li NMR spectra of 0.10 M solutions of [^{6}Li]**2** (**A**) and [^{6}Li]**1** (**B**) in 0.50 M Et_2NH/toluene at -60 °C. The measured mole fractions of **A** in (a)-(e) are 1.00, 0.65, 0.47, 0.29, and 0.00, respectively.

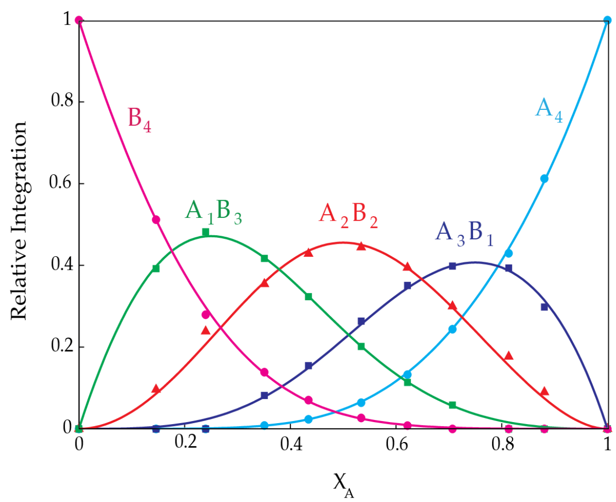

Figure 67. Job plot showing the relative integrations versus the measured mole fractions of **2** for 0.10 M mixtures of [^{6}Li]**2** (**A**) and [^{6}Li]**1** (**B**) in 0.50 M Et_2NH/toluene at -60 °C.

Trimer Job Plots in Diethylamine

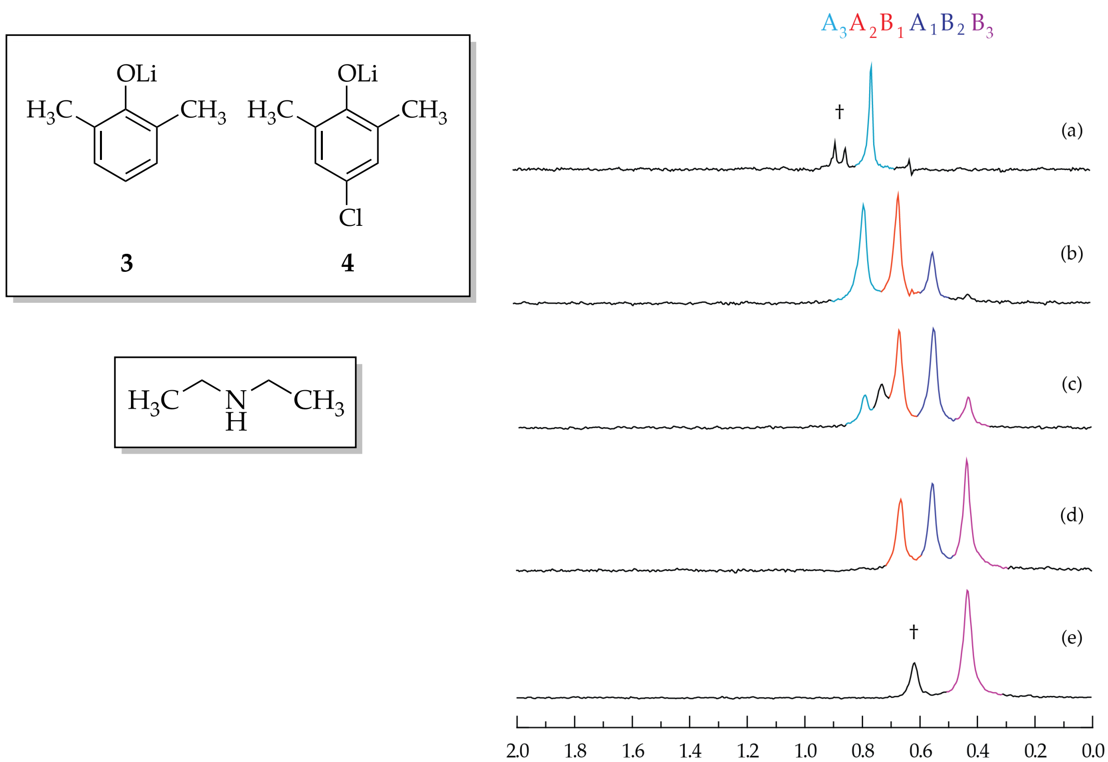

Figure 68. ^{6}Li NMR spectra of 0.10 M solutions of [^{6}Li]**3** (**A**) and [^{6}Li]**4** (**B**) in 0.50 M Et_2NH/toluene at -80 °C. The measured mole fractions of **A** in (a)-(e) are 1.00, 0.69, 0.53, 0.31, and 0.00, respectively. † indicates unknown aggregate.

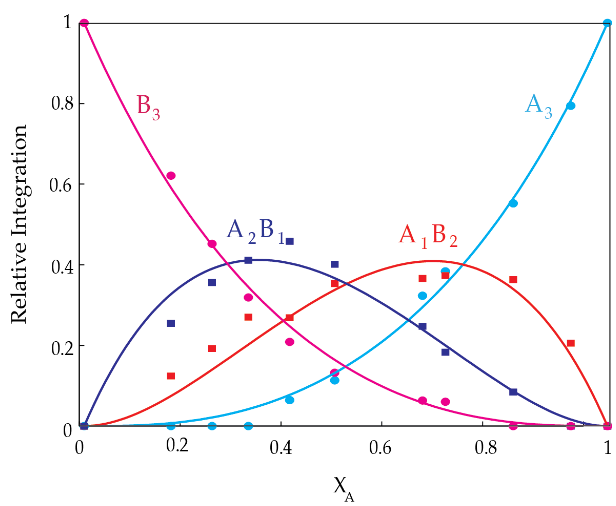

Figure 69. Job plot showing the relative integrations versus the measured mole fractions of **3** for 0.10 M mixtures of [^{6}Li]**3** (**A**) and [^{6}Li]**4** (**B**) in 0.50 M Et_2NH/toluene at -80 °C.

Tetramer Job Plots in *n*-Dipropylamine

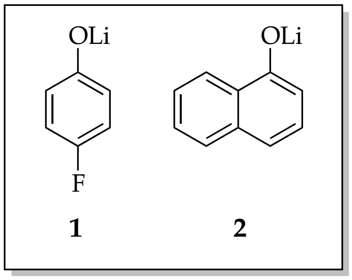

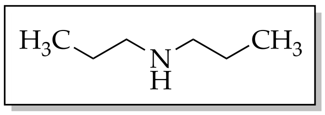

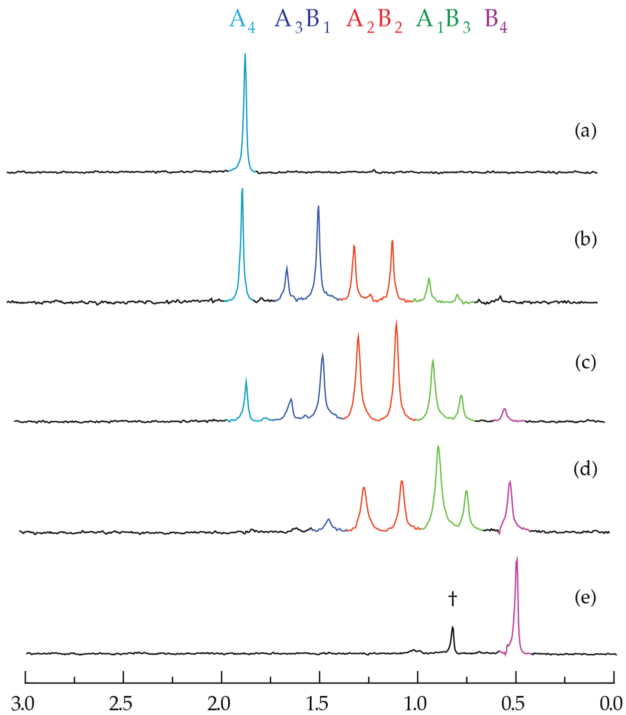

Figure 70. ^{6}Li NMR spectra of 0.10 M solutions of [^{6}Li]**2** (**A**) and [^{6}Li]**1** (**B**) in 0.50 M *n*-Pr_2NH/toluene at -80 °C. The measured mole fractions of **A** in (a)-(e) are 1.00, 0.68, 0.52, 0.31, and 0.00, respectively.

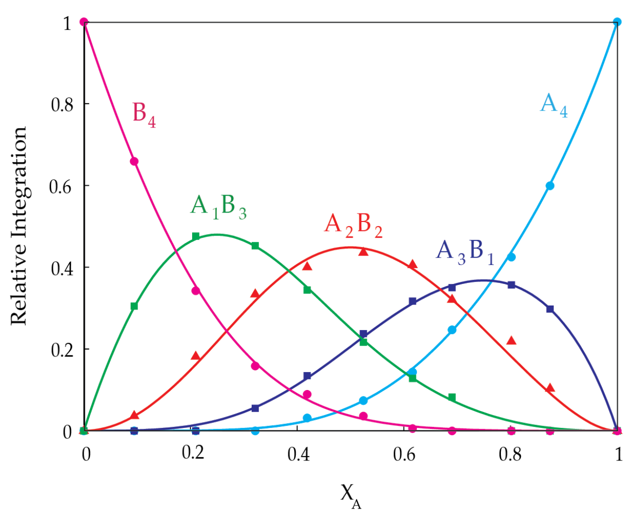

Figure 71. Job plot showing the relative integrations versus the measured mole fractions of **2** for 0.10 M mixtures of [^{6}Li]**2** (**A**) and [^{6}Li]**1** (**B**) in 0.50 M *n*-Pr_2NH/toluene at -80 °C.

Trimer Job Plots in *n*-Dipropylamine

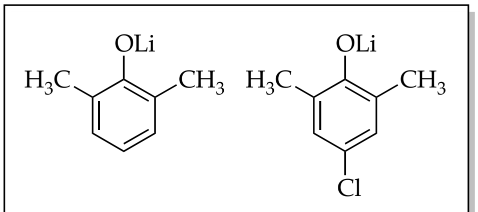

3 **4**

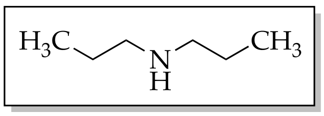

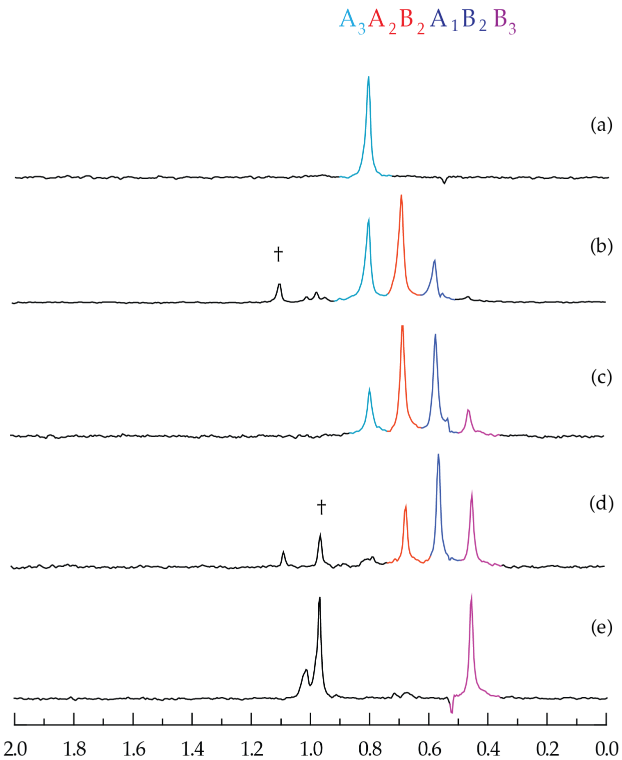

Figure 72. ^{6}Li NMR spectra of 0.10 M solutions of [^{6}Li]**3** (**A**) and [^{6}Li]**4** (**B**) in 0.50 M *n*-Pr_2NH/toluene at -80 °C. The measured mole fractions of **A** in (a)-(e) are 1.00, 0.62, 0.46, 0.27, and 0.00, respectively. † indicates unknown aggregate.

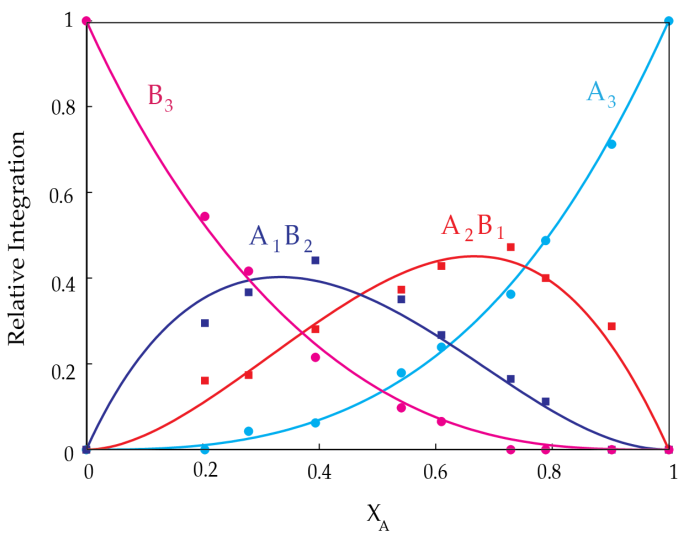

Figure 73. Job plot showing the relative integrations versus the measured mole fractions of **3** for 0.10 M mixtures of [^{6}Li]**3** (**A**) and [^{6}Li]**4** (**B**) in 0.50 M *n*-Pr_2NH/toluene at -80 °C.

<u>Tetramer Job Plots in *t*-Butanol</u>

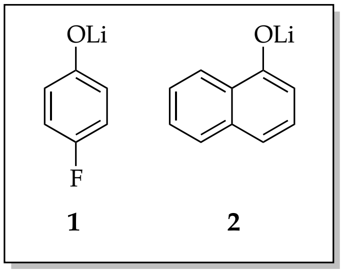

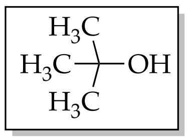

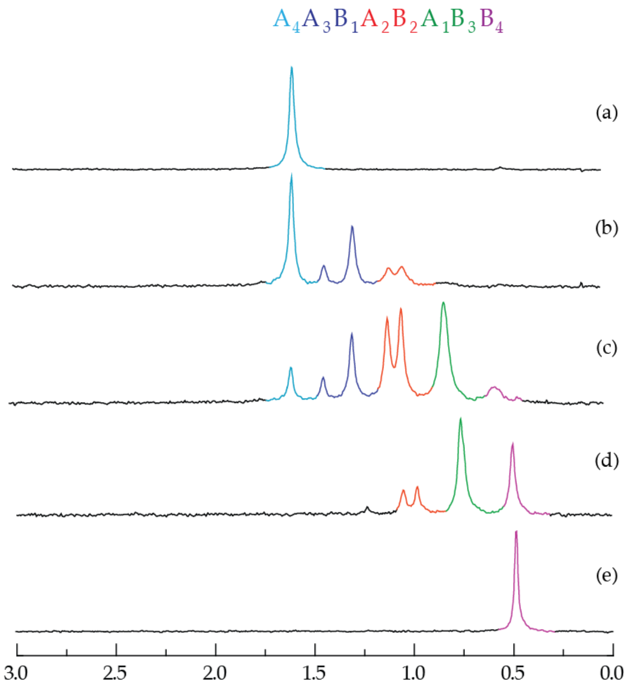

Figure 74. ^{6}Li NMR spectra of 0.10 M solutions of [^{6}Li]**2** (**A**) and [^{6}Li]**1** (**B**) in 0.50 M *t*-BuOH/toluene at -95 °C. The measured mole fractions of **A** in (a)-(e) are 1.00, 0.75, 0.41, 0.21, and 0.00, respectively.

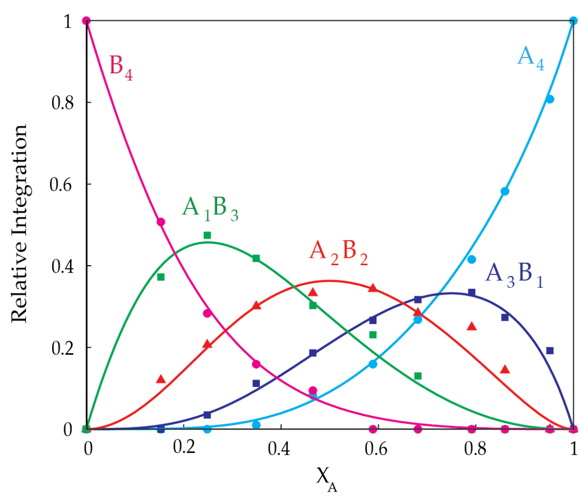

Figure 75. Job plot showing the relative integrations versus the measured mole fractions of **2** for 0.10 M mixtures of [^{6}Li]**2** (**A**) and [^{6}Li]**1** (**B**) in 0.50 M *t*-BuOH/toluene at -95 °C.

Tetramer Job Plots in *sec*-Butanol

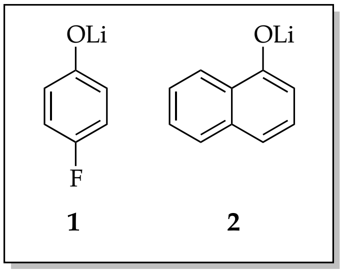

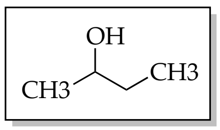

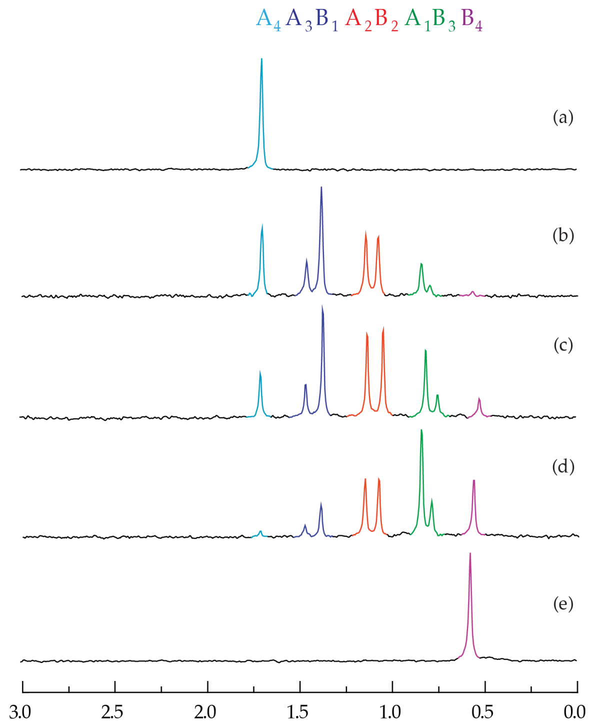

Figure 76. ^{6}Li NMR spectra of 0.10 M solutions of [^{6}Li]**2** (**A**) and [^{6}Li]**1** (**B**) in 0.50 M *sec*-BuOH/toluene at -80 °C. The mole fractions of **A** in (a)-(e) are 1.00, 0.65, 0.46, 0.27, 0.00, respectively.

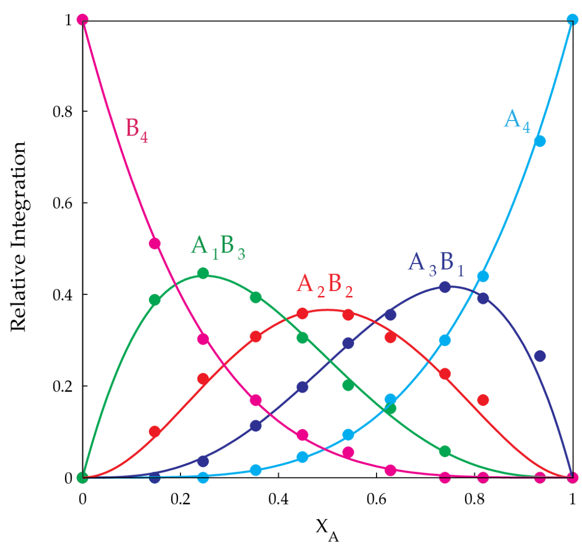

Figure 77. Job plot showing the relative integrations versus mole fractions of **2** for 0.10 M mixtures of [^{6}Li]**2** (**A**) and [^{6}Li]**1** (**B**) in 0.50 M *sec*-BuOH/toluene at -80 °C.

^{6}Li Spectra in *n*-Butanol

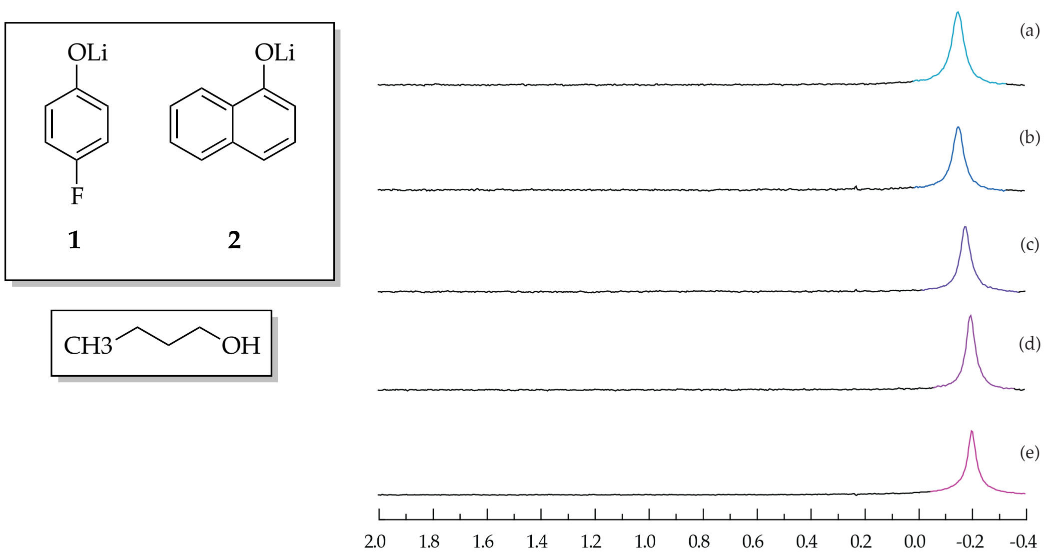

Figure 78. ^{6}Li NMR spectra of 0.10 M solutions of [^{6}Li]**2** (a) and [^{6}Li]**1** (e) in 0.50 M *n*-BuOH/toluene at -110 °C. The measured mole fractions cannot be calculated, but the mole fraction of **2** in tubes (b), (c), and (d) are roughly 0.75, 0.50, and 0.25, respectively.

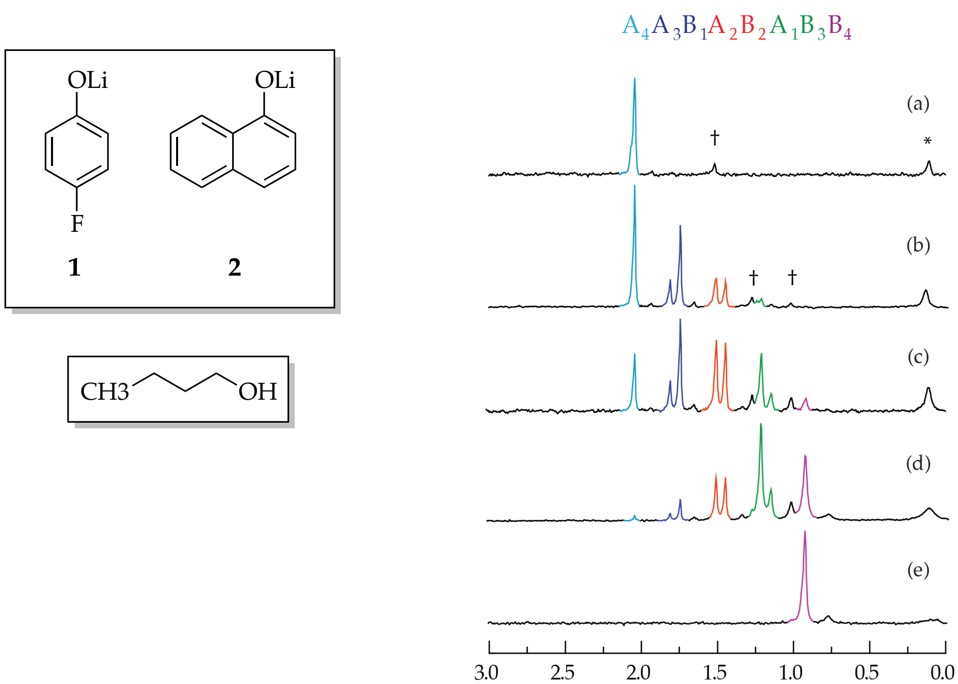

Figure 79. ^{6}Li NMR spectra of 0.10 M solutions of [^{6}Li]**2** (**A**) and [^{6}Li]**1** (**B**) in 0.50 M *n*-BuOH/ether at -60 °C. The mole fractions of **A** in tubes (a)-(e) are roughly 1.00, 0.75, 0.50, 0.25, 0.00, respectively. The ether cosolvent provides the aggregate resolution, however, *n*-BuOH has been shown to bind to lithium preferentially over ether. † denotes unknown aggregate. * denotes ^{6}LiHMDS.

Solvent Swap

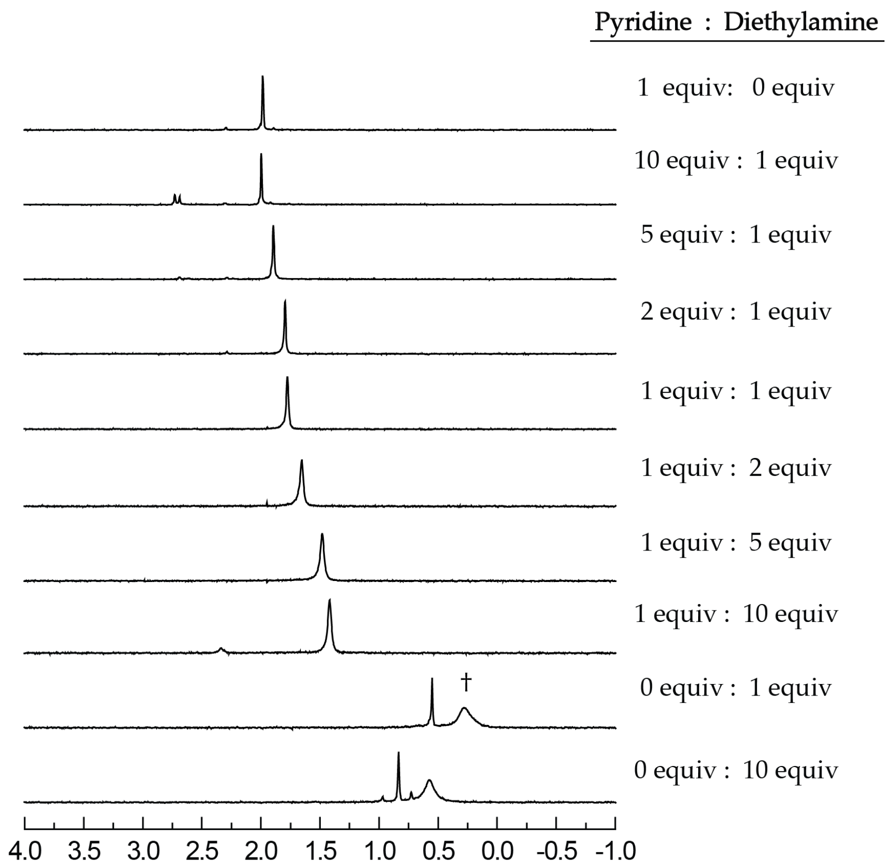

Figure 80. Solvent swap on 0.10 M of [^{6}Li]**1** in various pyridine and Et_2NH concentrations with toluene as cosolvent at -80 °C. The chemical shift more closely resembles pyridine even at high Et_2NH concentrations. The peak migration, however, indicates that Et_2NH is also functioning as a ligand to the tetramer. The medium dependent chemical shift is clearly demonstrated going from 1.0 equiv to 10 equiv of Et_2NH. † denotes unknown aggregate.

Solvent Swap

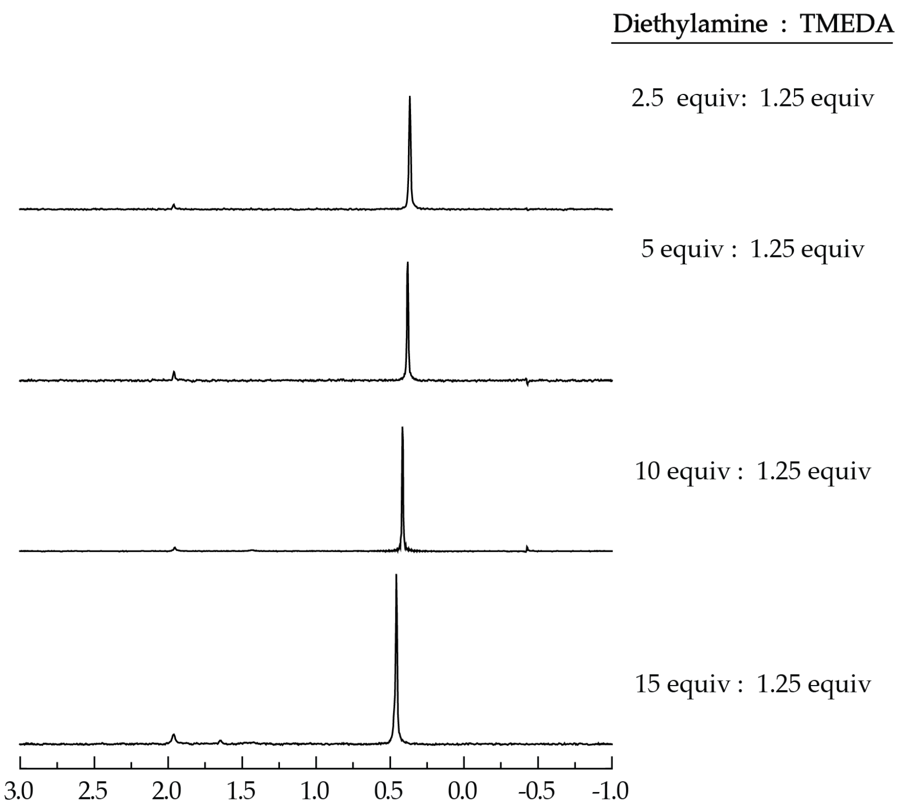

Figure 81. Solvent swap on 0.10 M of [^{6}Li]**2** in various ratios of Et_2NH and TMEDA with toluene as cosolvent at -40 °C. Addition up to 15 equiv of Et_2NH does not move the naphtholate aggregate from being solely a TMEDA-bound dimer.

Solvent Swap

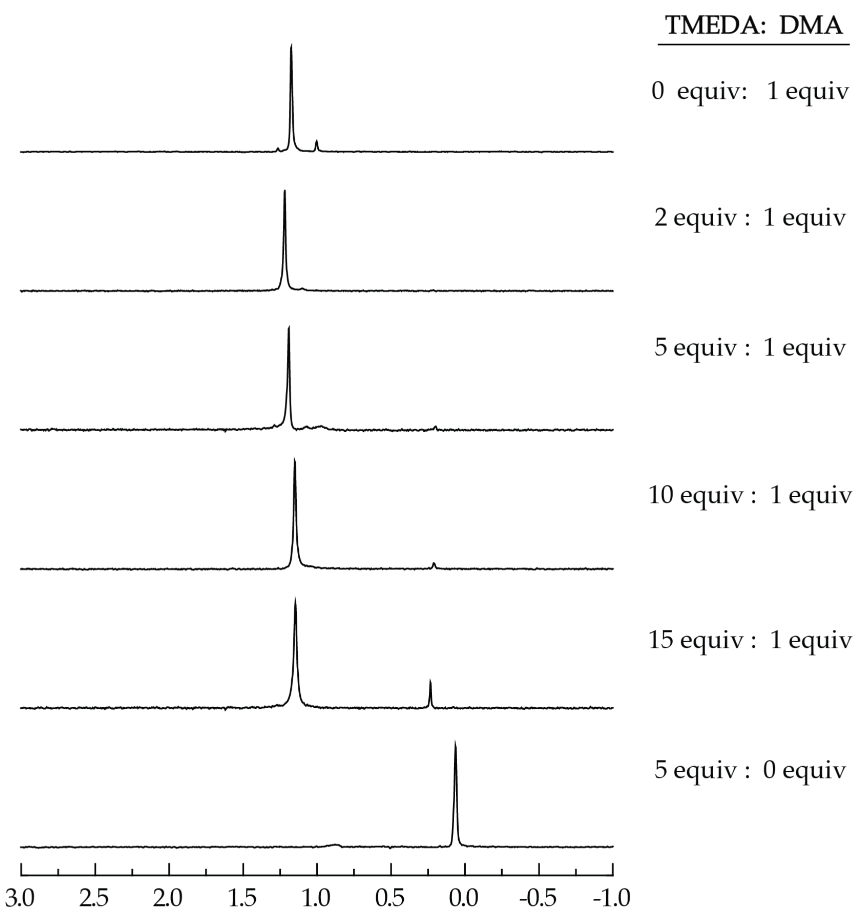

Figure 82. Solvent swap on 0.10 M of [^{6}Li]**1** in 1 equiv dimethylacetamide and various TMEDA concentrations with toluene as cosolvent at -80 °C. Addition of up to 15 equiv of TMEDA does not affect the chemical shift, indicting that the tetramer is solely DMA-bound. The appearance of a small peak at high TMEDA concentrations may be the concentration-dependent chemical shift of the TMEDA-solvated dimer.

Solvent Swap

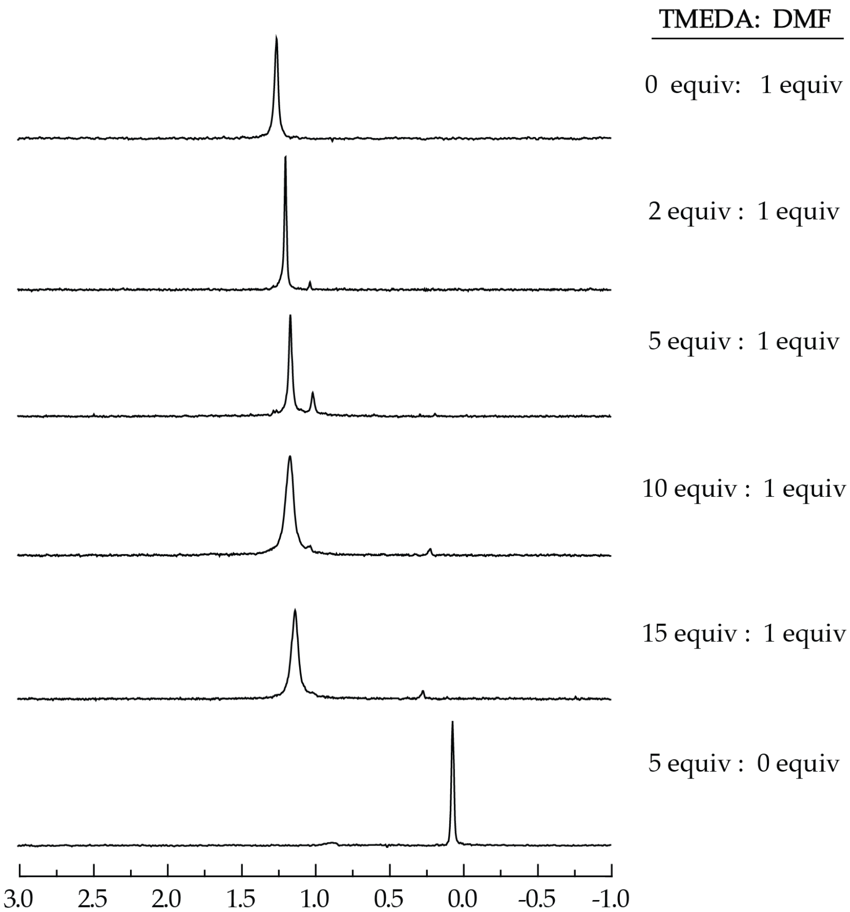

Figure 83. Solvent swap on 0.10 M of [^{6}Li]**1** in 1 equiv dimethylformamide and various TMEDA concentrations with toluene as cosolvent at -80 °C. Addition of up to 15 equiv of TMEDA does not affect the chemical shift, indicting the tetramer is solely DMF-bound. The appearance of a small blip at high TMEDA concentrations may be the concentration-dependent chemical shift of the TMEDA-solvated dimer.

Solvent Swap

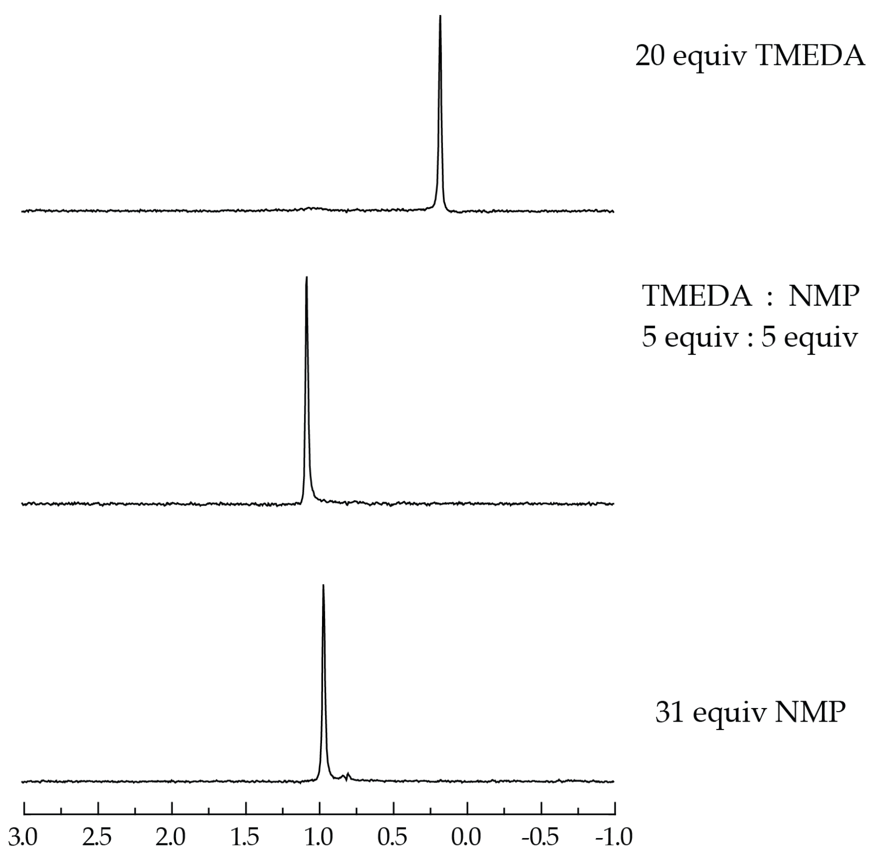

Figure 84. Solvent swap on 0.10 M of [^{6}Li]**1** in *N*-methylpyrrolidone and TMEDA with toluene as cosolvent at -80 °C. At a 1:1 ligand ratio, the chemical shift closely resembles the chemical shift of NMP, indicating that it is solely a NMP bound tetramer. The slight chemical shift difference is probably due to the difference in ligand concentration (medium effect).

Solvent Swap

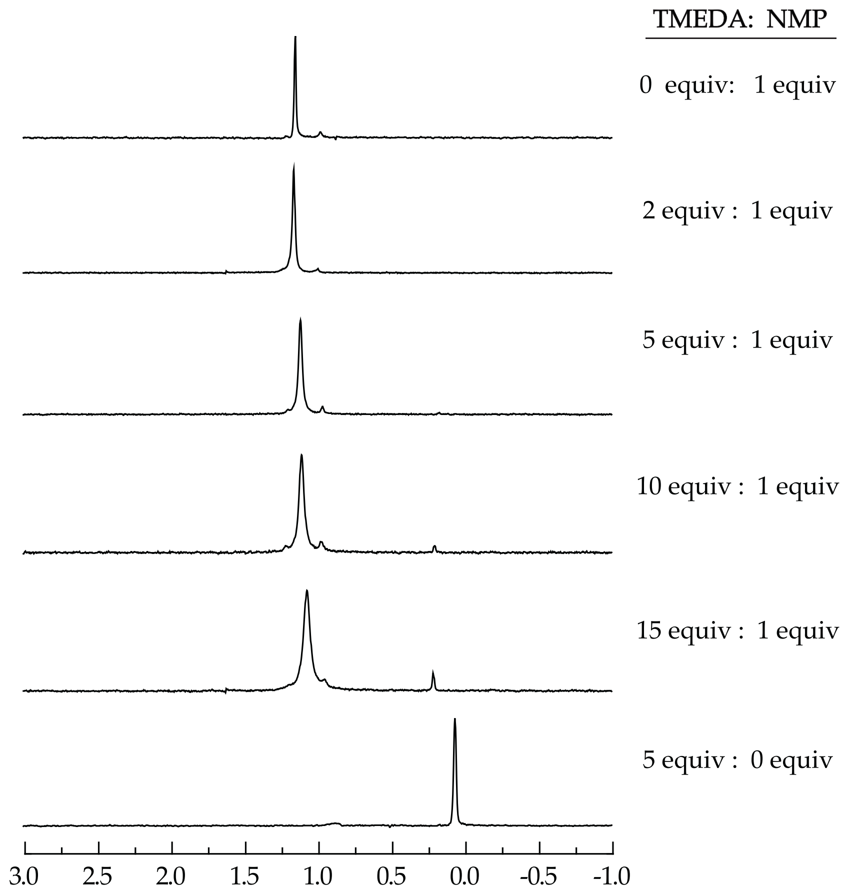

Figure 85. Solvent swap on 0.10 M of [^{6}Li]**1** in 1 equiv *N*-methylpyrrolidone and various TMEDA concentrations with toluene as cosolvent at -80 °C. Addition of up to 15 equiv of TMEDA does not affect the chemical shift, indicting the tetramer is solely NMP-bound. The appearance of a small peak at high TMEDA concentrations may be the concentration-dependent chemical shift of the TMEDA-solvated dimer.

Solvent Swap

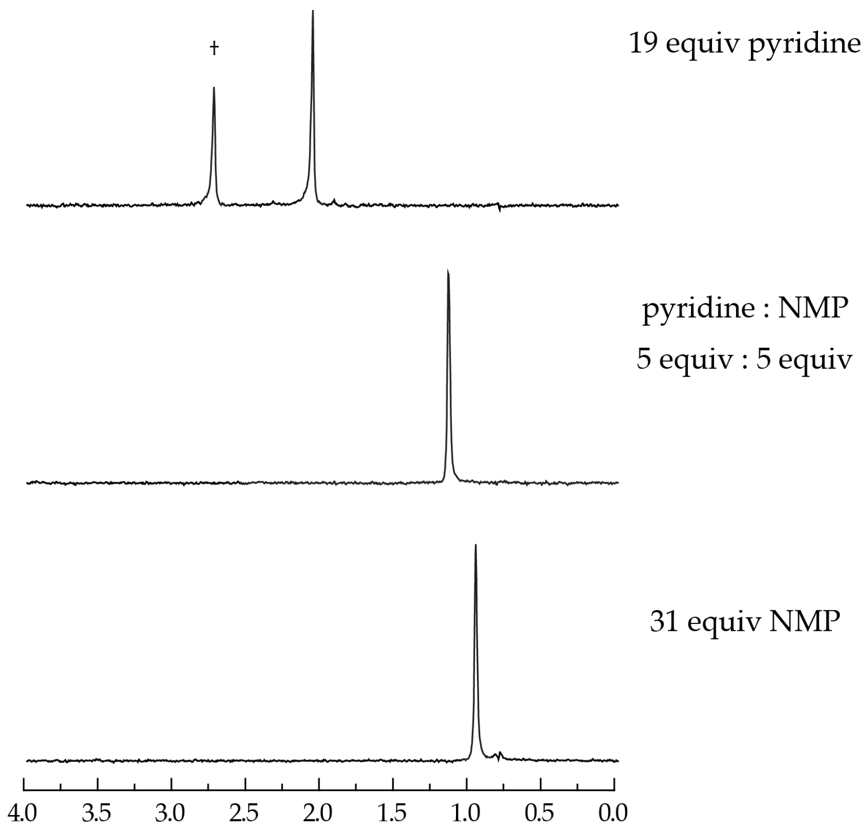

Figure 86. Solvent swap on 0.10 M of [^{6}Li]**1** in pyridine and *N*-methylpyrrolidone with toluene as cosolvent at -80 °C. At a 1:1 ligand ratio, the chemical shift closely resembles the chemical shift of NMP, indicating that it is predominantly a NMP bound tetramer. The slight chemical shift difference may be due to minor pyridine binding. † denotes an aggregate present only at high pyridine concentration; it is assumed to be a highly solvated dimer.

Solvent Swap

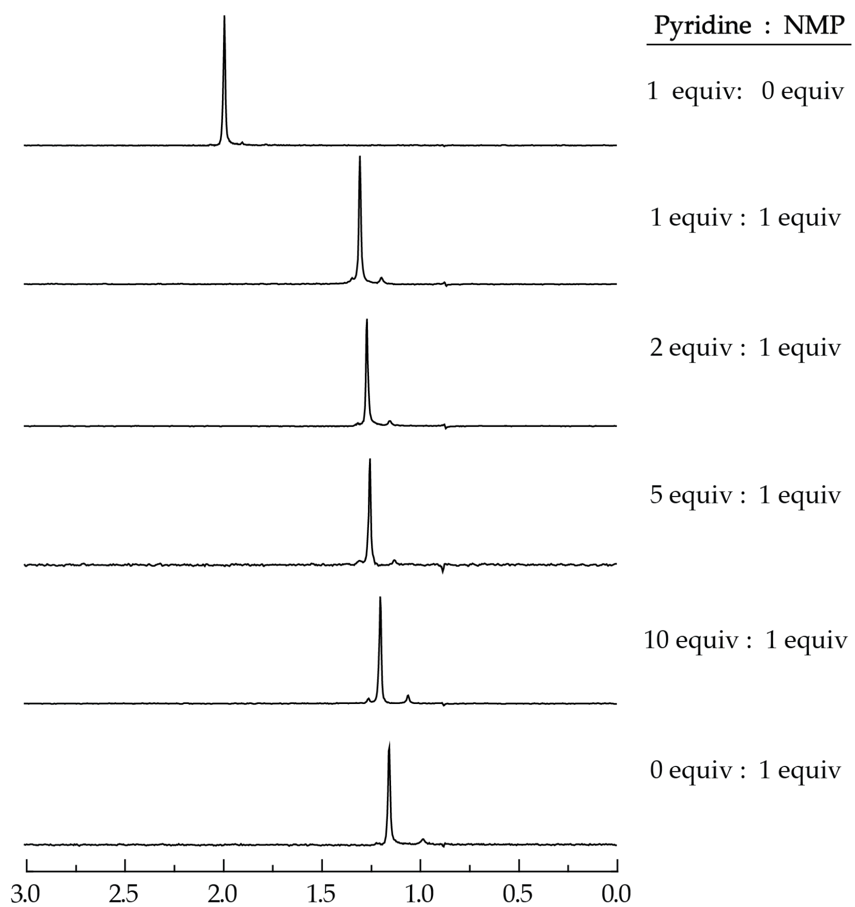

Figure 87. Solvent swap on 0.10 M of [^{6}Li]**1** in 1 equiv *N*-methylpyrrolidone and various pyridine concentrations with toluene as cosolvent at -80 °C. Addition of up to 10 equiv of pyridine does not affect the chemical shift, indicting the tetramer is solely NMP-bound.

Solvent Swap

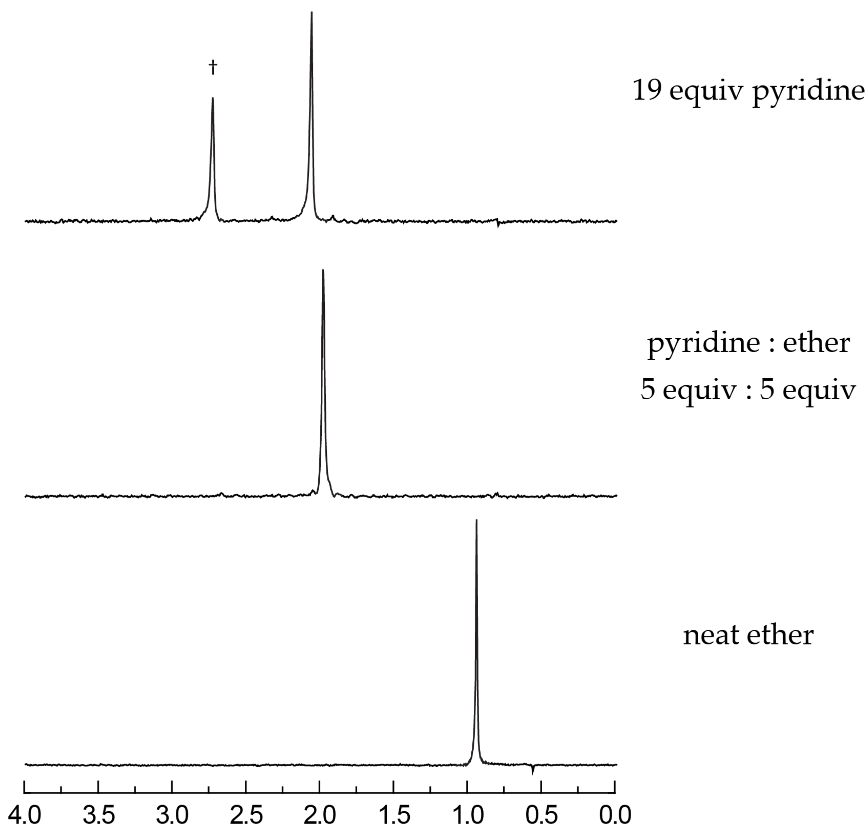

Figure 88. Solvent swap on 0.10 M of [^{6}Li]**1** in pyridine and diethyl ether with a toluene cosolvent as needed at -40 °C. At a 1:1 ligand ratio, the chemical shift closely resembles the chemical shift of pyridine, indicating that it is predominantly a pyridine bound tetramer. The slight chemical shift difference may be due to minor ether binding. † denotes an aggregate present only at high pyridine concentration; it is assumed to be a highly solvated dimer.

Solvent Swap

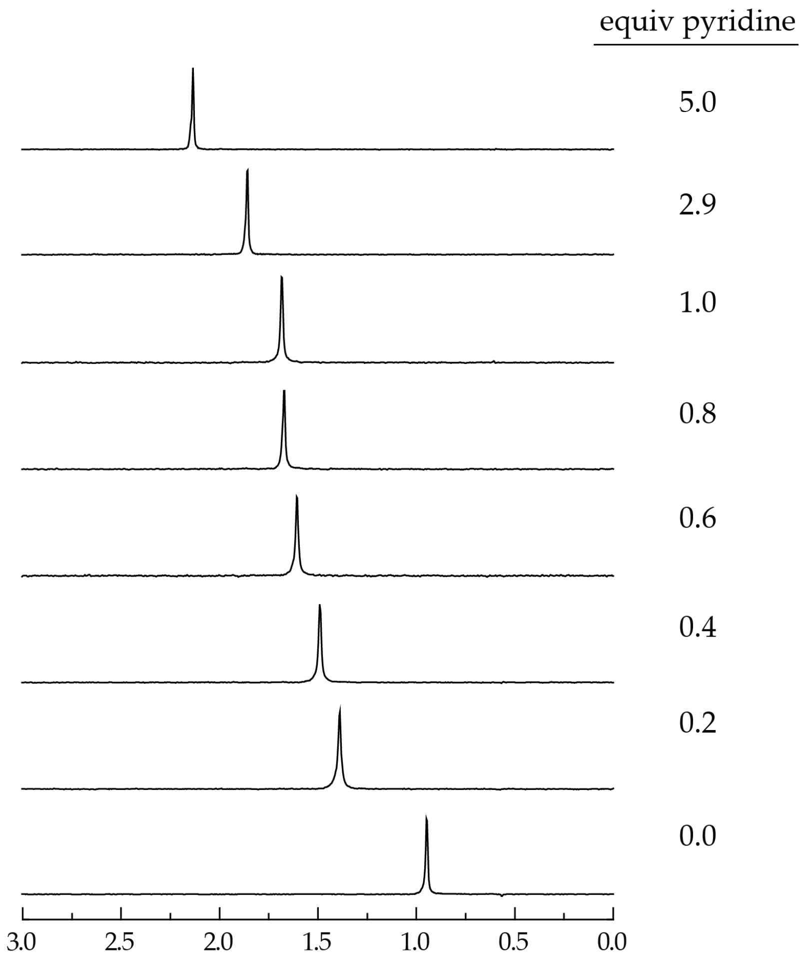

Figure 89. Solvent swap on 0.10 M of [^{6}Li]**1** in ether with increasing pyridine concentrations at -40 °C. Using ether as the cosolvent enables ether to compete with pyridine as the ligand for the tetramer.

Solvent Swap

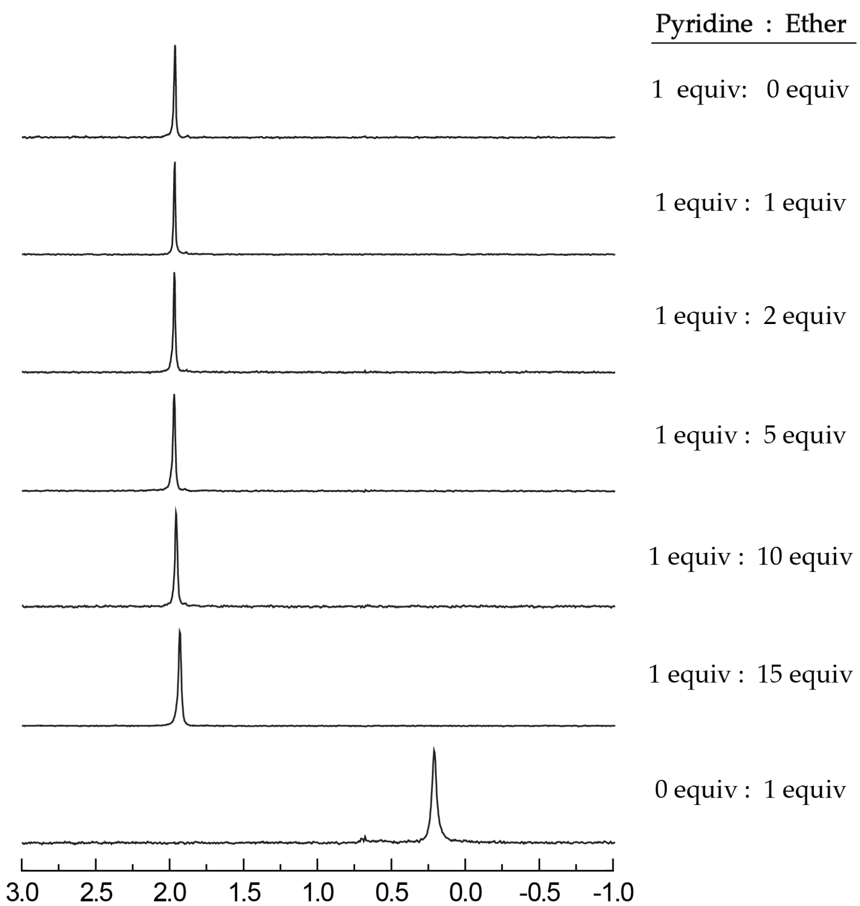

Figure 90. Solvent swap on 0.10 M of [^{6}Li]**1** in toluene with 1 equiv pyridine and increasing Et_2O concentrations at -80 °C. Up to 15 equiv of Et_2O yields no impact on the pyridine-solvated tetramer.

Solvent Swap

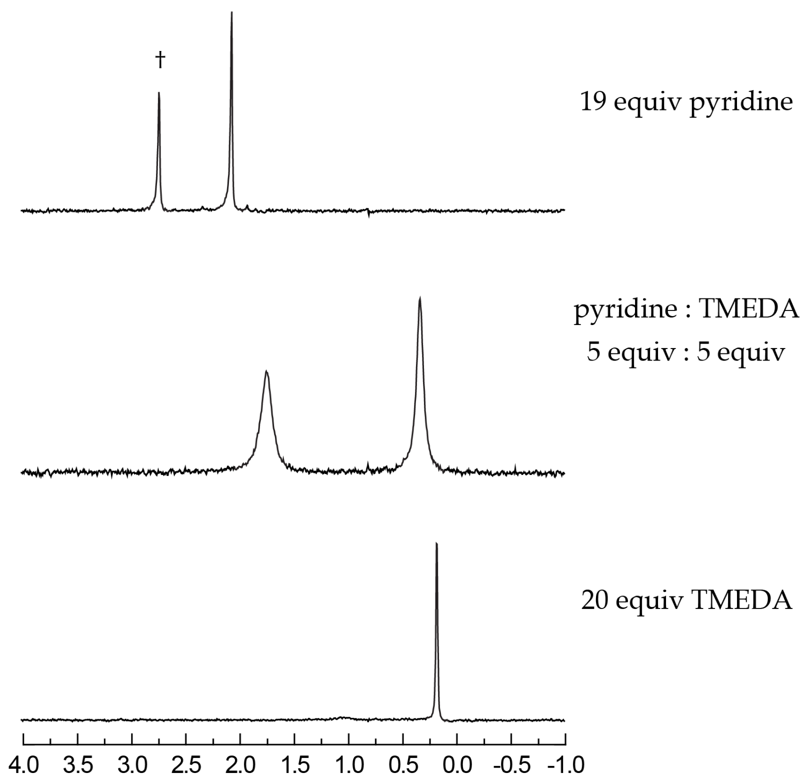

Figure 91. Solvent swap on 0.10 M of [^{6}Li]**1** in pyridine and TMEDA with toluene as cosolvent at -40 °C. At a 1:1 ligand ratio, there is broadening and minor inward shift of both the pyridine solvated tetramer and the TMEDA solvated dimer. This change indicates the possibility of mixed ligand aggregates. † denotes an aggregate present only at high pyridine concentration; it is assumed to be a highly solvated dimer.

Solvent Swap

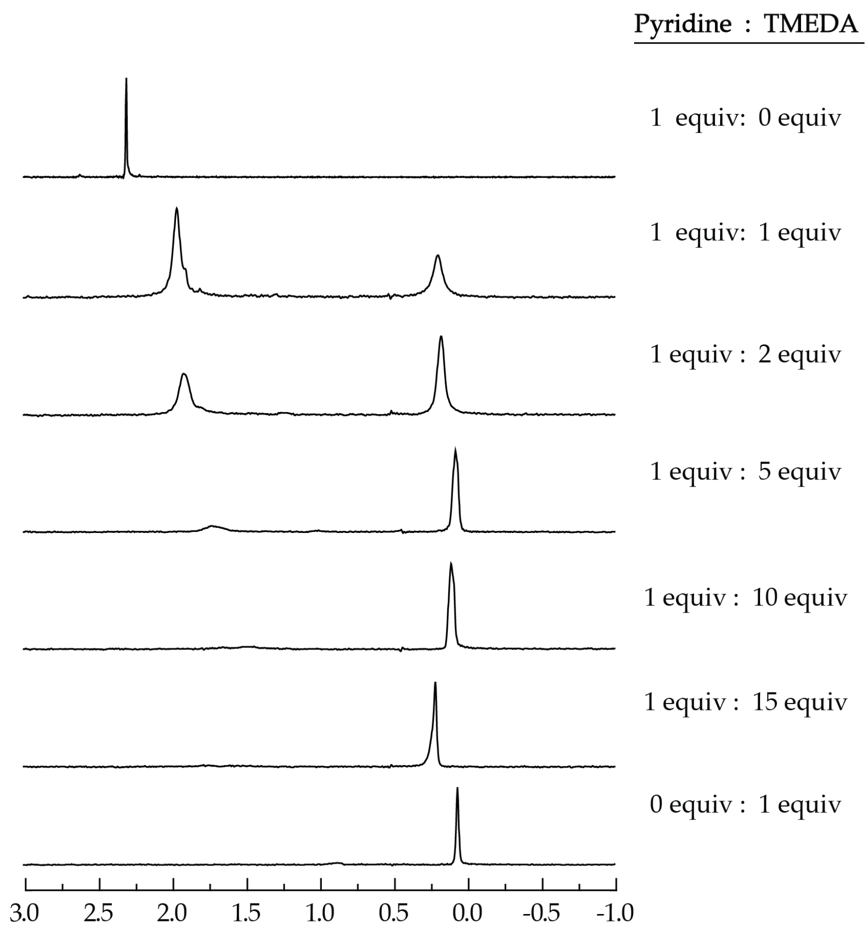

Figure 92. Solvent swap on 0.10 M of [^{6}Li]**1** in pyridine and various TMEDA concentrations with toluene as cosolvent at -80 °C. Addition of TMEDA causes both the appearance of a TMEDA solvated dimer around 0.2 ppm and a slight shift of the pyridine solvated tetramer. The slight shift may be due to incorporation of TMEDA into the tetramer. The chemical shift variation at increasing TMEDA concentration is due to a medium effect.

Solvent Swap

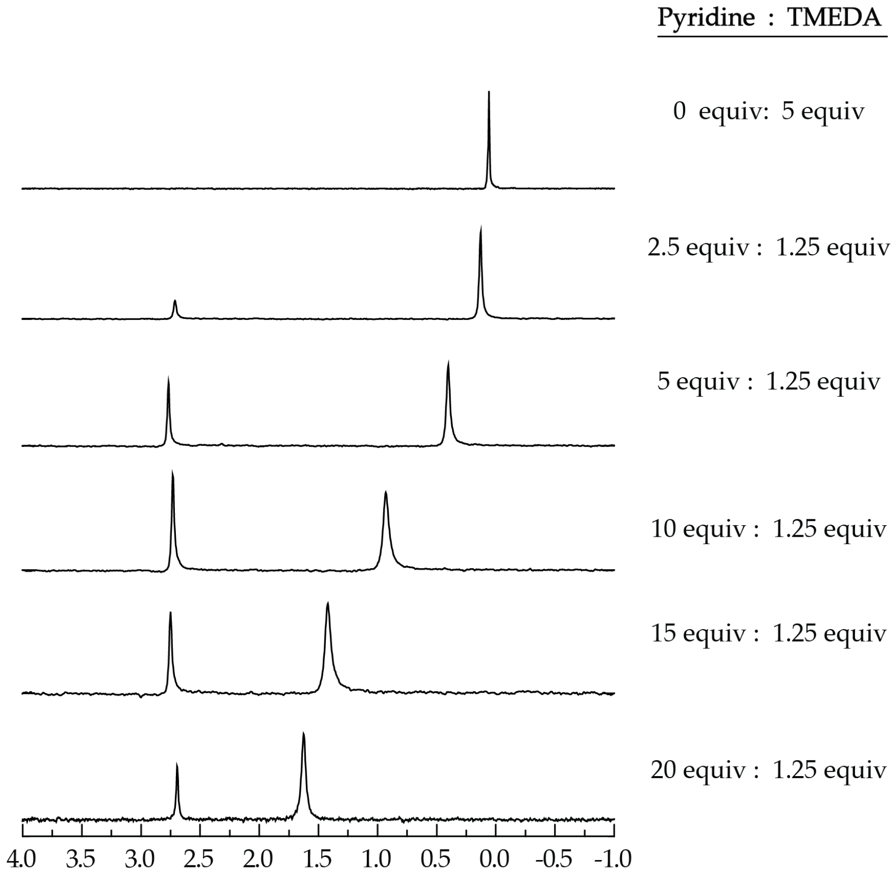

Figure 93. Solvent swap on 0.10 M of [^{6}Li]**2** in TMEDA and various pyridine concentrations with toluene as cosolvent at -40 °C. Addition of pyridine causes both the appearance of a pyridine solvated tetramer around 2.75 ppm and the migration of the TMEDA solvated dimer.

Solvent Swap

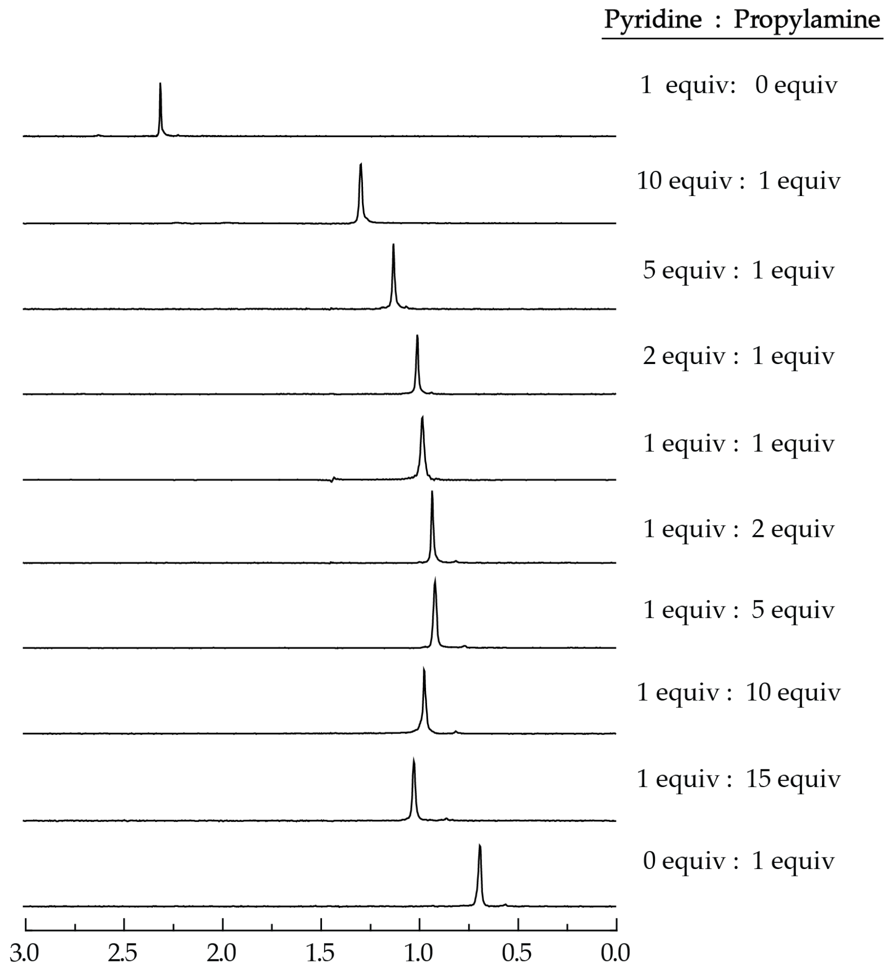

Figure 94. Solvent swap on 0.10 M of [^{6}Li]**1** in various pyridine and *n*-PrNH concentrations with toluene as cosolvent at -80 °C. The chemical shift more closely resembles *n*-PrNH even at high pyridine concentrations. The medium dependent chemical shift is clearly demonstrated going from 1.0 equiv to 15 equiv of *n*-PrNH.

Solvent Swap

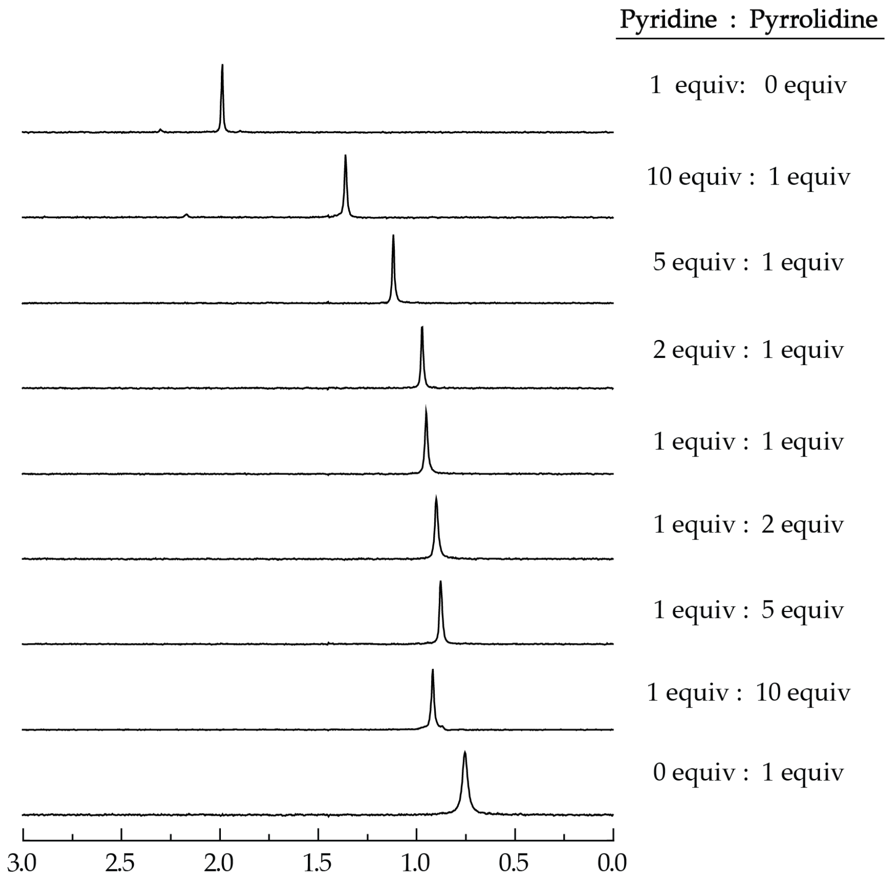

Figure 95. Solvent swap on 0.10 M of [^{6}Li]**1** in various pyridine and pyrrolidine concentrations with toluene as cosolvent at -80 °C. The chemical shift more closely resembles pyrrolidine even at high pyridine concentrations. The medium dependent chemical shift is clearly demonstrated going from 1.0 equiv to 10 equiv of pyrrolidine.

Solvent Swap

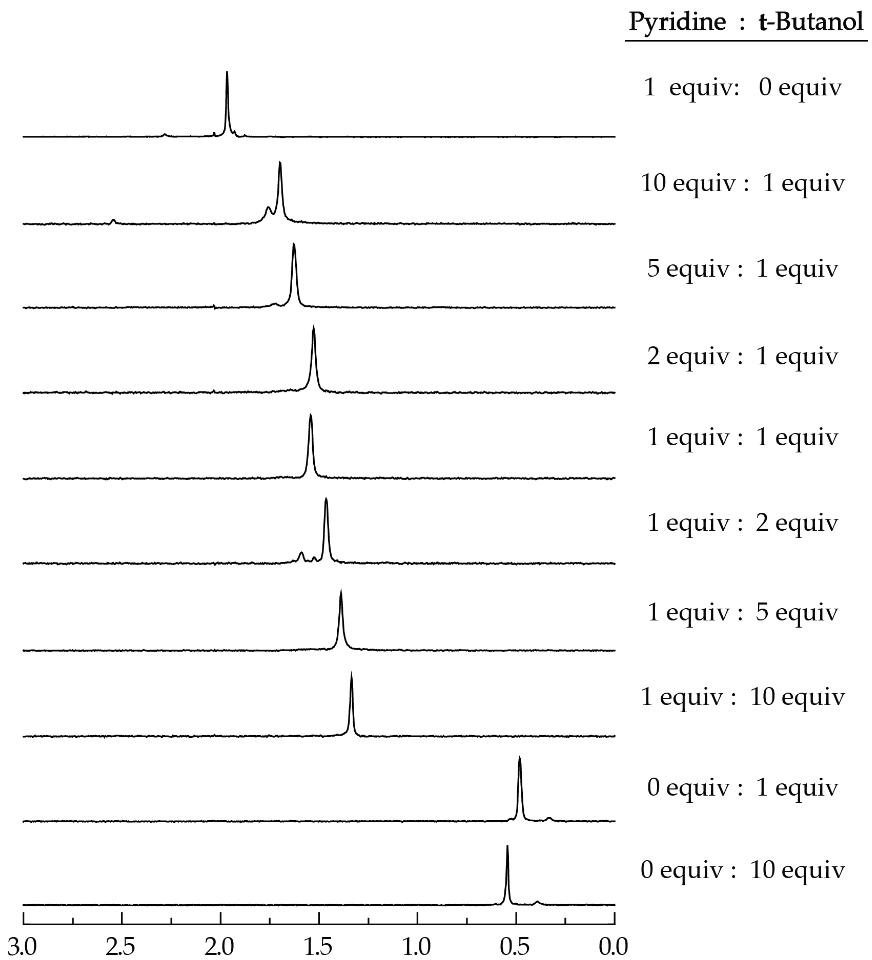

Figure 96. Solvent swap on 0.10 M of [^{6}Li]**1** in various pyridine and *t*-BuOH concentrations with toluene as cosolvent at -80 °C. The chemical shift more closely resembles pyridine even at high *t*-BuOH concentrations. The medium dependent chemical shift is barely present going from 1.0 equiv to 10 equiv of *t*-BuOH.